iScience

CellPress
OPEN ACCESS

Article

Celecoxib alleviates pathological cardiac hypertrophy and fibrosis via M1-like macrophage infiltration in neonatal mice

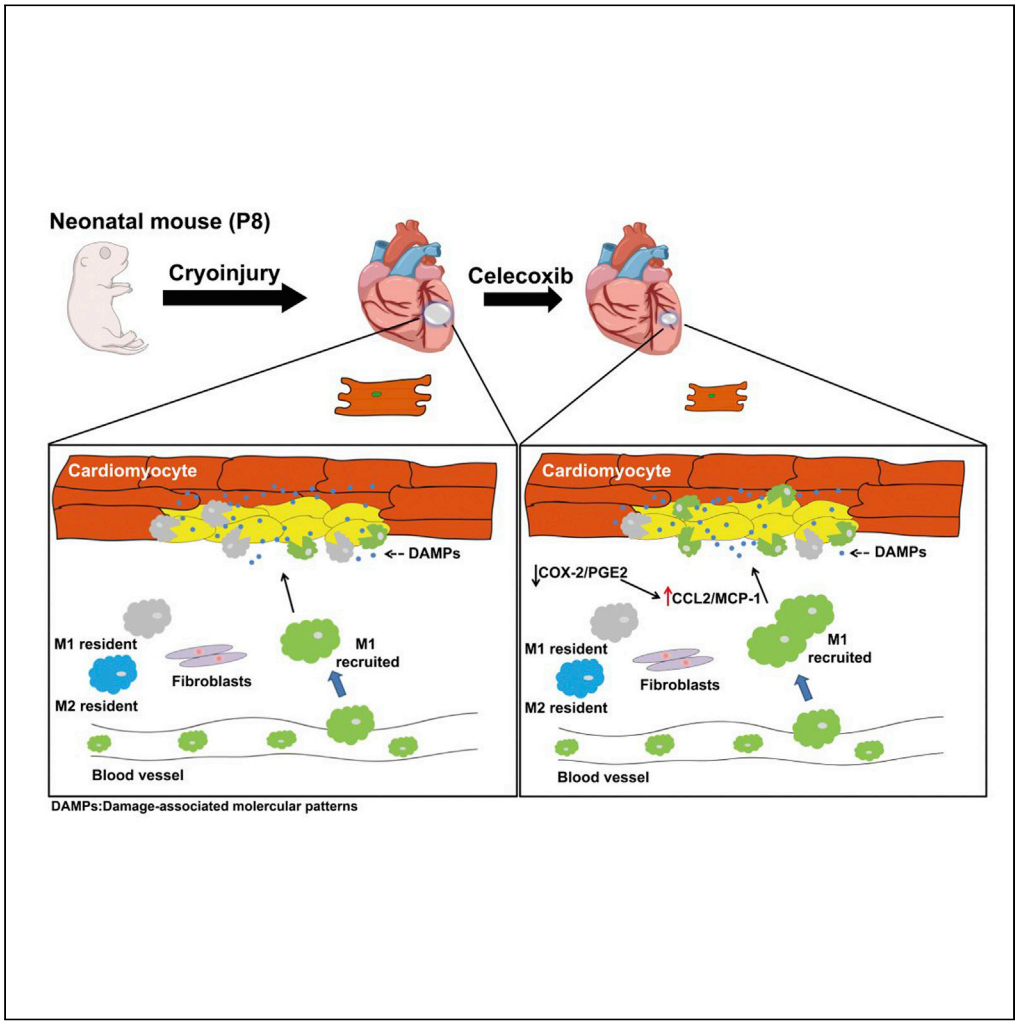

Yanli Zhao, Qi Zheng, Hanchao Gao, Mengtao Cao, Huiyun Wang, Rong Chang, Changchun Zeng

yanlizhao2015@126.com (Y.Z.)
zengchch@glmc.edu.cn (C.Z.)

HIGHLIGHTS

Cryoinjury successfully induces cardiac hypertrophy and fibrosis in P8 ICR mice

COX-2 inhibition alleviates cardiac hypertrophy and fibrosis after cryoinjury

MCP-1 significantly increases in COX-2 inhibition

COX-2 inhibition improves cardiac repair in P8 ICR mice by recruiting M1-like macrophages

Zhao et al., iScience 24, 102233
March 19, 2021 © 2021 The Authors.
https://doi.org/10.1016/j.isci.2021.102233

iScience

CellPress
OPEN ACCESS

Article

Celecoxib alleviates pathological cardiac hypertrophy and fibrosis via M1-like macrophage infiltration in neonatal mice

Yanli Zhao,[1,4,*] Qi Zheng,[2] Hanchao Gao,[1] Mengtao Cao,[1] Huiyun Wang,[1] Rong Chang,[1,3] and Changchun Zeng[1,*]

SUMMARY

Cardiac hypertrophy is an adaptive response to all forms of heart disease, including hypertension, myocardial infarction, and cardiomyopathy. Cyclooxygenase-2 (COX-2) overexpression results in inflammatory response, cardiac cell apoptosis, and hypertrophy in adult heart after injury. However, immune response-mediated cardiac hypertrophy and fibrosis have not been well documented in injured neonatal heart. This study showed that cardiac hypertrophy and fibrosis are significantly attenuated in celecoxib (a selective COX-2 inhibitor)-treated P8 ICR mice after cryoinjury. Molecular and cellular profiling of immune response shows that celecoxib inhibits the production of cytokines and the expression of adhesion molecular genes, increases the recruitment of M1-like macrophage at wound site, and alleviates cardiac hypertrophy and fibrosis. Furthermore, celecoxib administration improves cardiac function at 4 weeks after injury. These results demonstrate that COX-2 inhibition promotes the recruitment of M1-like macrophages during early wound healing, which may contribute to the suppression of cardiac hypertrophy and fibrosis after injury.

INTRODUCTION

Myocardial infarction (MI) is the leading cause of mortality. The process of MI contributes to pathological cardiac hypertrophy, including individual cardiomyocyte enlargement and increase in left ventricular wall thickness (Nakamura and Sadoshima, 2018). During cardiac hypertrophy, a series of pathological changes occur, such as cardiomyocyte death, cardiac muscle contraction, dilated cardiomyocytes, and other cardiac diseases, which contribute to heart dysfunction. Non-regenerating mice (P7, at postnatal day 7) lack regenerative capacity with age; thus immune cells (e.g., CD4+ T cells, regulatory T cells, and macrophages) and non-immune cells (e.g., cardiac fibroblast, cardiac endothelial cells, and remaining cardiomyocytes) are important mediators of cardiac hypertrophy and fibrosis after injury (Frieler and Mortensen, 2015; Kvakan et al., 2009; Lai et al., 2019; Ma et al., 2019). In addition, hypertrophic gene expression and inflammatory response have been reported during cardiac fibrosis (Manabe et al., 2002). Thus, deciphering the role of immune response mediating cardiac fibrosis could provide novel insights into cardiac hypertrophy after injury.

Selective cyclooxygenase-2 inhibitors are non-steroidaal anti-inflammatory drugs belonging to the COX family (cyclooxygenase-1 [COX-1], cyclooxygenase-2 [COX-2], and cyclooxygenase-3 [COX-3]) for acute or chronic inflammation and pain in clinical settings (Nissen et al., 2016). Inducible COX-2 is increased in inflammatory diseases, transplantation, and heart diseases with inflammation progress, such as airway inflammation (Rumzhum and Ammit, 2016), chronic pancreatitis (Huang et al., 2019), diabetes (Robertson, 2017), hypertension (Wong et al., 2013), cardiac allograft transplantation (Yang et al., 2000), and coronary artery disease (Chenevard et al., 2003). Upregulated COX-2 and its products also contribute to vascular dysfunction and heart failure after injury. In vascular endothelial cells, COX-2 inhibitor attenuates C-reactive protein (CRP) and inhibits interleukin-6 (IL-6) and tissue factor production (Al-Rashed et al., 2018;(Steffel et al., 2005) Chenevard et al., 2003). In cardiac function, COX-2 inhibitors reduce myocardial damage and inflammation after cardiac allograft transplantation (Ma et al., 2002). Intriguingly, COX-2 inhibitors or knockout mice improve cardiac hypertrophy and dysfunction after injury or stimulation in different adult models, such as MI, ischemia with reperfusion, abdominal aortic constrictions, and Ang II- and aldosterone-induced cardiac hypertrophy (Camitta et al., 2001; Chi et al., 2017; Feniman De Stefano et al., 2016; Wu et al., 2005; Zhang et al., 2016).

[1]Department of Medical Laboratory, Shenzhen Longhua District Central Hospital, Affiliated Central Hospital of Shenzhen Longhua District, Guangdong Medical University, Shenzhen 518110, China

[2]School of Life Sciences, Shandong University, Qingdao 266237, China

[3]Department of Cardiovascular Medicine, Shenzhen Longhua District Central Hospital, Affiliated Central Hospital of Shenzhen Longhua District, Guangdong Medical University, Shenzhen 518110, China

[4]Lead contact

*Correspondence: yanlizhao2015@126.com (Y.Z.), zengchch@glmc.edu.cn (C.Z.)

https://doi.org/10.1016/j.isci.2021.102233

This is an open access article under the CC BY-NC-ND license (http://creativecommons.org/licenses/by-nc-nd/4.0/).

After injury, pro-inflammatory response suppresses wound healing because of the migration and recruitment of many inflammatory cells at the wound site (Epelman et al., 2015). Anti-inflammatory regulatory cells contribute to heart regeneration and cardiac cell survival, such as regulatory macrophages, Tregs, and invariant natural killer T cells (Aurora et al., 2014; Homma et al., 2013; Sobirin et al., 2012; Zacchigna et al., 2018). Emerging studies have shown that macrophages play a vital role in tissue regeneration after injury (Aurora et al., 2014; Simoes et al., 2020; Wynn and Vannella, 2016). Macrophages induce angiogenesis after MI, promoting cardiac regeneration in mice (Aurora et al., 2014). Consequently, macrophages enhance collagen deposition and fibrosis to scar formation in non-regenerating mice (Simoes et al., 2020). Macrophages also secrete cytokines (TNF-α, IL-1β, and IL-10), matrix metallopeptidase, chemokines (CCL2, CCR7, CXCL9, and CXCL10), and growth factors (transforming growth factor [TGF-β], vascular endothelial growth factor, epidermal growth factor, and fibroblast growth factor) to promote or inhibit wound healing (Braga et al., 2015; Ding et al., 2019; Mantovani et al., 2004). Interestingly, COX-2 regulates pro-inflammatory and anti-inflammatory responses to modulate tissue repair (Kaushik and Das, 2019; Li et al., 2018). Recent studies have shown that celecoxib (a selective cyclooxygenase-2 inhibitor) reduces the production of pro-inflammatory cytokines (TNF-α, IL-6, IL-1β, and IL-17), iNOS expression, and the recruitment of F4/80 + macrophages and CD4+ T cells, thereby promoting wound healing in skin repair (Geesala et al., 2017; Romana-Souza et al., 2016). Low levels of COX-2 and PGE_2 also limit scar formation in fetal skin wound by reducing TGF-β1 expression and suppressing inflammatory response (Wilgus et al., 2004). Intriguingly, emerging studies demonstrated that COX-2 deficiency or inhibition can reduce myocardial fibrosis, infarcted myocardial wall thickness, and infarct collagen density in mice (Chi et al., 2017; LaPointe et al., 2004). In neonatal rat model, COX-2 expression is associated with endothelin-1-induced cardiac hypertrophy *in vitro* (Li et al., 2014). Although low levels of COX-2 enhance tissue healing, promotion of scar-free heart repair using selective COX-2 inhibition remains unclear in neonatal mice.

Also, accumulating studies have reported that neonatal mice provided an ideal model in which to demonstrate tissue repair or regeneration because neonatal mice have remarkable regenerating or repairing capacity compared with adult mice (Konfino et al., 2015; Mahmoud et al., 2014; Porrello et al., 2011; Xia et al., 2018). A recent study reported that cryoinjury (CI) induced successful cardiac hypertrophy in GATA4 knockout neonatal mice, but not apical resection injury model (Yu et al., 2016). Also, no blood loss, scaling injury size (e.g., 0.5 mm, 1.0 mm, and 2.0 mm), and reproducible results could be useful for the comparison between regenerative and non-regenerative neonatal models in CI model (Polizzotti et al., 2015, 2016). Thus, we used CI injury neonatal model to induce cardiac hypertrophy and fibrosis in our study. In this study, we found that celecoxib treatment attenuated pro-inflammatory cytokine production, hypertrophic and pro-fibrotic gene expression, and adhesion molecule gene expression in neonatal non-regenerative heart following CI. We also demonstrated that selective COX-2 inhibition may induce M1-like macrophage infiltration, which improves cardiac hypertrophy and fibrosis at the early stage of heart injury in non-regenerative mice.

RESULTS

Different hypertrophic changes during neonatal mouse regeneration

We induced CI in regenerating (P3) and non-regenerating (P8) ICR mice to investigate whether or not different hypertrophic changes occur during heart regeneration (Figure 1A). Heart weight/body weight (HW/BW) (mg/g) and cardiomyocyte size (μm^2) were observed at 4 weeks after injury in the P3 and P8 groups. Surprisingly, the HW/BW and cardiomyocyte size of the injured P8 hearts from the border zone significantly increased compared with those of the sham group and P3 injured hearts, and the injured P3 hearts even showed obvious scar formation (Figures 1B–1E). In line with previous studies (Cui et al., 2020; Wang et al., 2019b), we also performed Masson's trichrome staining to identify cardiac fibrosis. Results showed that collagen content significantly increased at 4 weeks after CI in P8 group compared with the P3 group (Figures 1E and 1F). Furthermore, we performed severe CI (copper wire: 2 mm^2) to induce cardiac hypertrophy of P3 and P8 group, demonstrating that HW/BW (mg/g) and collagen content of P8 CI group significantly increased compared with that of sham and P3 CI group (Figures S1A–S1C). Also, the percentage of relative wall thickness was higher in the P8 group than in the P3 group at 4 weeks after injury (Figures S1D and S1E). These data showed that non-regenerating mice showed cardiac hypertrophic changes and failed to regenerate in the infarct zone after injury.

Inflammatory stimuli change during neonatal mouse regeneration

To determine whether or not inflammatory stimuli are involved in cardiac hypertrophy and fibrosis, we performed real-time PCR to identify the changes in inflammatory stimuli in the infarct zone between the P3 and

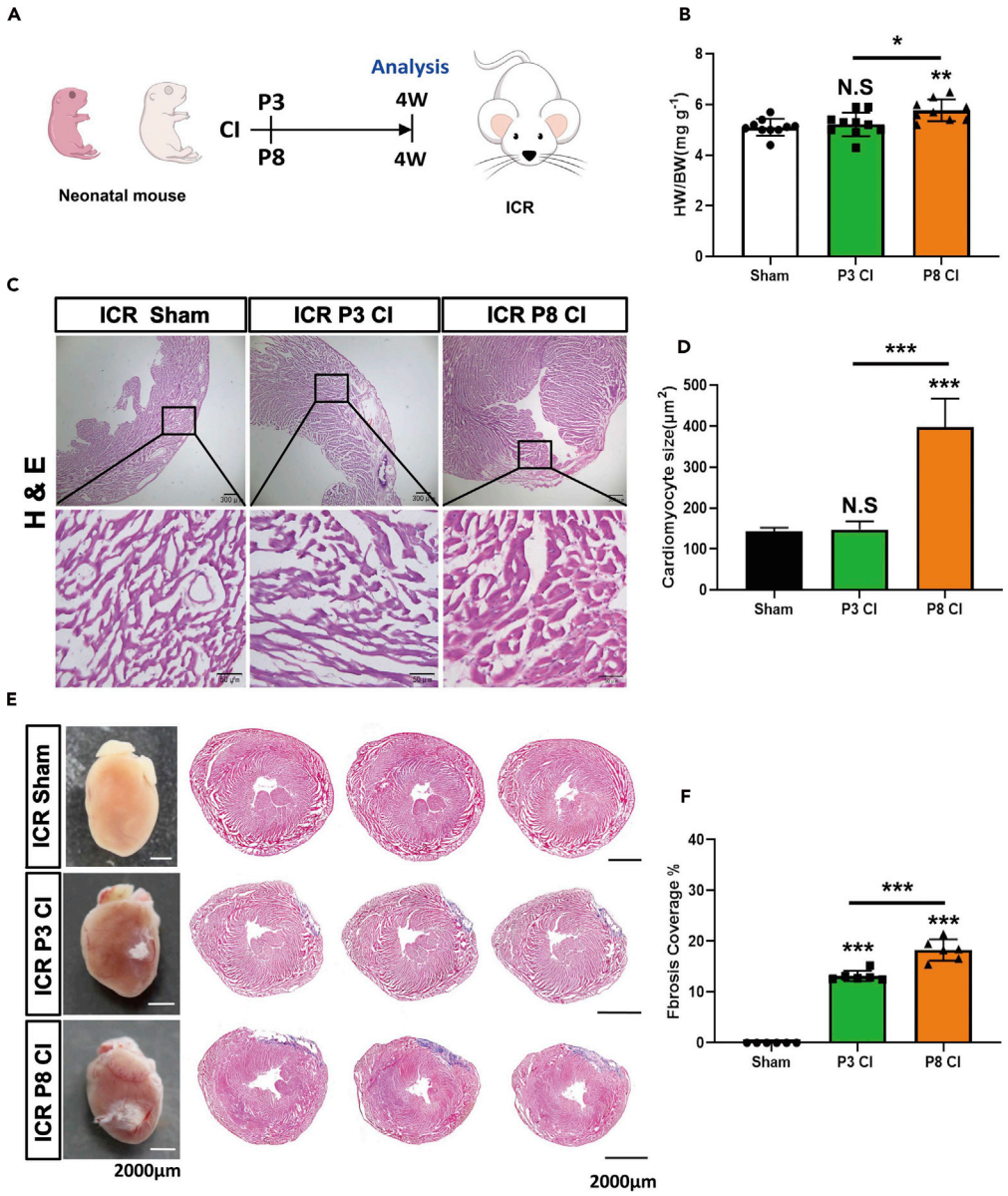

Figure 1. Cardiac hypertrophy and fibrosis were induced in non-regenerative mice (P8) following CI

(A) Experimental design of cryoinfarction (cryoinjury [CI]) injury model and analysis in (B–F).

(B) Heart weight/body weight (HW/BW, mg/g) in sham, regenerating mice (P3, at postnatal day 3), and non-regenerating mice (P8) at 4 weeks after injury.

(C) Heart tissue of sham, P3 injury, and P8 injury was cross-sectioned and stained with hematoxylin and eosin (H&E) for analysis; scale bars: 300 μm (40× objective) and 50 μm (400× objective);

(D) Quantification of sham, P3, and P8 cardiomyocytes at 4 weeks after injury (n = 3 per group, independent experiments [n = 2]).

(E) Heart tissue of P3 or P8 after injury (copper wire area: 1 mm^2, ICR mother mice: 4–6 weeks) was stained with Masson's trichrome; scale bar, 2,000 μm.

(F) Quantification of fibrosis coverage (%, 100 × scar perimeter/total perimeter) in P3 and P8 left ventricle at 4 weeks following CI. Data are representative of two independent experiments (n = 4–6 per group, mean ± SD. *$p < 0.05$, **$p < 0.01$, ***$p < 0.001$)

Table 1. Listing of primers and primer sequences for real-time PCR

No.	Gene name	Primer sequence (5′–3′)
1	COX-2	TGCTGTACAAGCAGTGGCAA
		GCAGCCATTTCCTTCTCTCC
2	IFN-γ	TCAAGTGGCATAGATGTGGAAGAA
		TGGCTCTGCAGGATTTTCATG
3	TNF-α	ATTATGGCTCAGGGTCCAAC
		GACAGAGGCAACCTGACCAC
4	IL-6	GACTTCCATCCAGTTGCCTT
		ATGTGTAATTAAGCCTCCGACT
5	IL-1β	GCTGCTTCCAAACCTTTGACC
		AGCCACAATGAGTGATACTGCC
6	IL-10	ATCTTAGCTAACGGAAACAACTCCT
		TAGAATGGGAACTGAGGTATCAGAG
7	IL-17	GCTGACCCCTAAGAAACCCC
		GAAGCAGTTTGGGACCCCTT
8	IL-21	GGCTCTCGTTCCCACAGATG
		CGTCTATAGTGTCCGGCGTC
9	VCAM-1	GCCACCCTCACCTTAATTGCT
		GCACACGTCAGAACAACCGAA
10	ICAM-1	CTCACTTGCAGCACTACGG
		TTCATTCTCAAAACTGACAGGC
11	MCP-1	TTAAAAACCTGGATCGGAACCAA
		GCATTAGCTTCAGATTTACGGGT
12	Myh-7	TGCCCCATATATACAGCCCCT
		TGGAGCCCCTTATCCCAGAG
13	Acta1	CGCCAGCCTCTGAAACTAGA
		ACGATGGATGGGAACACAGC
14	Nppb (BNP)	TTTGGGCTGTAACGCACTGA
		CACTTCAAAGGTGGTCCCAGA
15	Nppa (ANP)	CTGCTTCGGGGGTAGGATTG
		CACACCACAAGGGCTTAGGA
16	TGF-β1	GGCCAGATCCTGTCCAAGC
		GTGGGTTTCCACCATTAGCAC
17	TGF-β2	CTTCGACGTGACAGACGCT
		GCAGGGGCAGTGTAAACTTATT
18	TGF-β3	CCTGGCCCTGCTGAACTTG
		TTGATGTGGCCGAAGTCCAAC
19	TGF-βr1	GAGATTCCAGCTGTTGTTCTGTTAT
		CTGTACTGCACTCCCAAACTATTCT
20	GAPDH	GGCATTGCTCTCAATGACAA
		TGTGAGGGAGATGCTCAGTG

P8 groups at 7 days or 4 weeks after injury (primers listed in Table 1). The mRNA and protein levels of COX-2 were significantly upregulated in the non-regenerative mice (P8) at 7 days and 4 weeks after injury (Figures 2A and 2B). The levels of IL-6, IL-10, IFN-γ, IL-17, and IL-21 also increased in the P3 and P8 groups at 4 weeks after CI compared with the sham group (Figure 2C). Meanwhile, the level of MCP-1 was significantly upregulated in both groups (Figure 2D). Moreover, the expression of adhesion molecular genes (VCAM-I and ICAM-I) was significantly increased (Figure 2D). Interestingly, the mRNA expression levels of IL-6, IL-1β, and

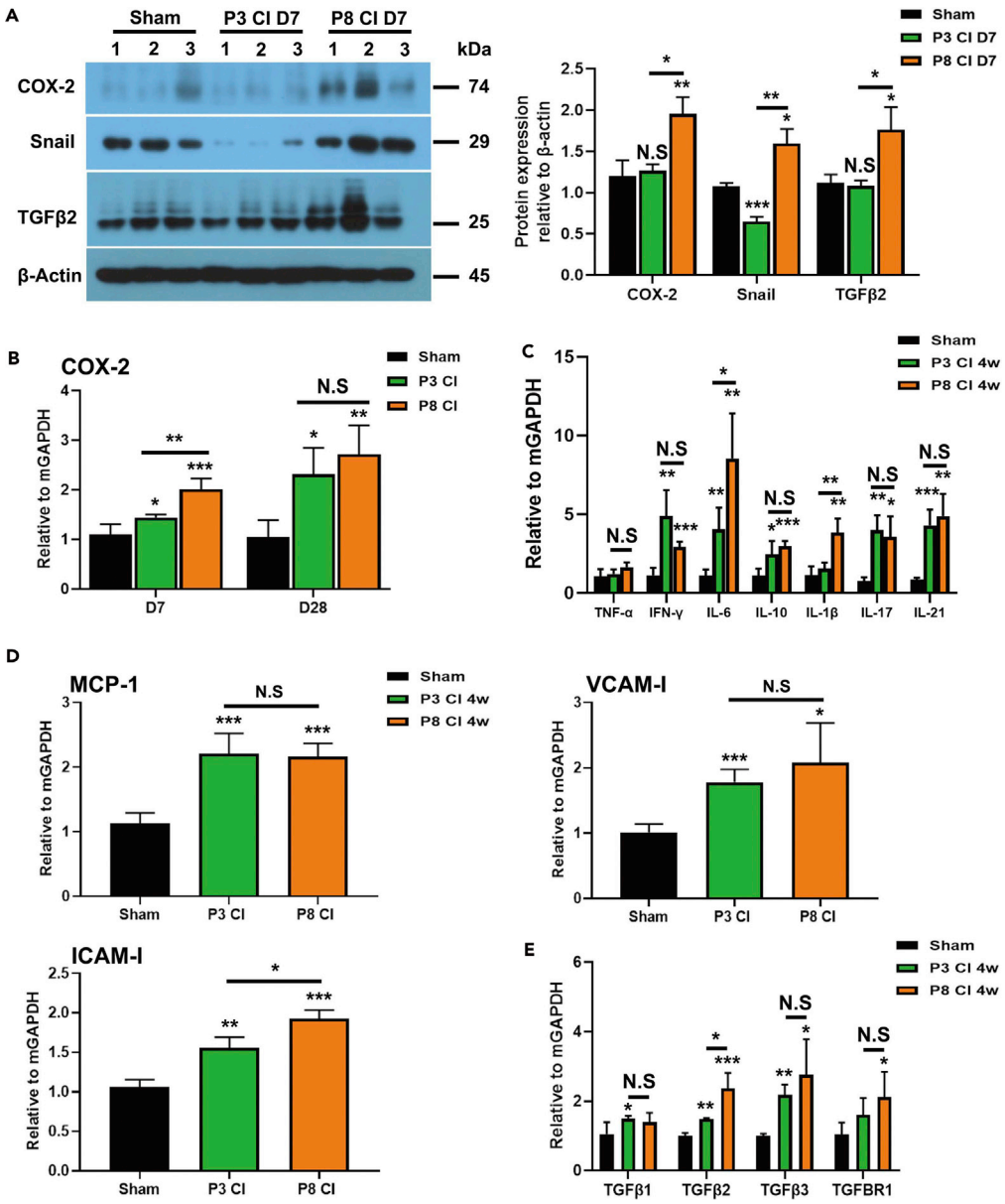

Figure 2. Pro-inflammatory cytokines, chemokines, and pro-fibrotic gene expression increased in P3 and P8 groups following CI

(A) Protein levels of COX-2, TGF-β2, and Snail in sham, P3, and P8 heart were measured using western blot at 7 days post CI, respectively;

(B–E) (B) mRNA level of COX-2 in Sham, P3, and P8 heart was measured using real-time PCR at 7 days and 4 weeks after injury; mRNA levels of (C) cytokines, (D) chemokines (MCP-1), adhesion molecular genes (ICAM-I and VCAM-I), and (E) pro-fibrotic genes (TGF-βs and TGFBR1) were measured using real-time PCR in Sham, P3, and P8 heart at 4 weeks after injury. Data are representative of two independent experiments (n = 4–6 per group, mean ± SD, *p < 0.05, **p < 0.01, ***p < 0.001).

ICAM-I significantly increased in the infarct zone of the P8 group than in that of the P3 group (Figures 2C and 2D).

In addition, we identified the mRNA levels of TGF-βs (1/2/3) at 4 weeks after CI as TGF-βs (1/2/3) are important mediators of cardiac hypertrophy and fibrosis (Kuwahara et al., 2002; Rosenkranz et al., 2002; Sakata et al., 2008). The mRNA levels of TGF-βs (1/2/3) and TGFBR1 were upregulated in both groups at 4 weeks

after CI, but no significant changes besides TGF-β2 were found in the infarct zone of P8 compared with P3 injured heart (Figure 2E). Furthermore, the protein levels of TGF-β2 and TGF-β signaling-induced Snail were increased in the P8 CI group at day 7 (Figure 2A).

These data demonstrated that inflammatory stimuli were induced in regenerating and non-regenerating hearts after injury, but IL-6, IL-1β, ICAM-I, and pro-fibrotic cytokine (TGF-β2) may be the predominant stimuli in cardiac hypertrophy and fibrosis after injury in non-regenerating mice. However, the resource of these pro-inflammatory stimuli remains unclear because various cell types produce different pathological stimuli after injury (Mahdavian Delavary et al., 2011; Manabe et al., 2002). Intriguingly, COX-2 inhibitors have been reported in suppressing or reducing cardiac hypertrophy and fibrosis in adult rat or mice after injury (Jacobshagen et al., 2008; Zhang et al., 2016). Celecoxib is a selective COX-2 inhibitor that has been approved for clinical use, and clinical trials showed that moderate doses of celecoxib exert no severe cardiovascular side effects (Slomski, 2016).

Celecoxib treatment inhibits cardiac hypertrophy and fibrosis after CI in non-regenerating mice

To investigate the role of celecoxib in cardiac hypertrophy and fibrosis in P8 after injury, we performed CI to P8 ICR mice treated or untreated with celecoxib (50 mg/kg) at days 0, 1, and 2 (Figure 3A). The ratio of HW/BW (mg/g) significantly increased in the untreated and treated P8 groups after injury compared with the sham group at 4 weeks (Figures 3B and 3C). Surprisingly, the HW/BW ratio significantly reduced in the celecoxib-treated P8 heart compared with the DMSO-treated P8 heart after injury at 4 weeks (Figures 3B and 3C). We also quantified the size of cardiomyocytes (μm^2) by using H&E and wheat germ agglutinin staining. Similarly, the size of cardiomyocytes from the border zone in P8 heart significantly reduced after celecoxib treatment compared with that of DMSO treatment at 4 weeks after injury, although the cardiomyocyte size of celecoxib-treated P8 CI heart was significantly increased compared with that of the sham group (Figure 3D). Meanwhile, we performed Masson's trichrome staining to identify the scar formation of P8 heart treated with DMSO and celecoxib at 4 weeks after injury. Celecoxib administration significantly reduced excessive scar formation in P8 heart (Figure 3E), which was completely different from adult heart after myocardial ischemia-reperfusion injury (Zhu et al., 2019). These data demonstrated that selective COX-2 inhibition would inhibit the cardiac hypertrophy and scar formation of non-regenerative mice (P8) when celecoxib is administrated at the early stage of injury.

Celecoxib inhibits hypertrophic and pro-fibrotic gene expression by regulating pro-inflammatory cytokines, chemokine (MCP-1), and adhesion molecule genes (ICAM-I and VCAM-I) after injury in non-regenerating mice

To study the changes in hypertrophic and pro-fibrotic gene expression after myocardial injury, we analyzed the published RNA-sequencing data in P1 and P8 at 1.5 and 7 days after MI, respectively (Wang et al., 2019b). In line with previous study, pro-inflammatory and pro-fibrotic signaling was induced in P8 heart compared with P1 heart at 1.5 and 7 days after injury (Wang et al., 2019b) (Figures S2A–S2C). To further demonstrate the relationship between inflammatory response and hypertrophy response, we reanalyzed related signaling pathways in regenerative and non-regenerative mice models at 7 days after injury. The Gene Ontology (GO) enrichment analysis showed that leukocyte migration, neutrophil migration, and cytokine- and chemokine-mediated signaling pathways were significantly enriched in the context of inflammatory response. Also, TGF-β signaling, PI3K-AKT signaling, extracellular matrix organization, hypertrophic cardiomyopathy, and collage fibril organization were significantly enriched, which may contribute to cardiac hypertrophy and fibrosis (Figure S2C). Furthermore, our bioinformatic analysis showed that the expression levels of hypertrophic genes (e.g., BNP, Myh7, and Acta1) and pro-fibrotic genes (e.g.,TGF-β1/2/3) significantly differed between regenerative and non-regenerative mice (Wang et al., 2019b) (Figure S2D). To study changes in hypertrophic genes, we identified cardiac hypertrophic makers through real-time PCR (primers listed in Table 1). The mRNA levels of ANP and Acta1 increased in P3 and P8 hearts at 7 days after injury, whereas those of BNP and Myh7 significantly increased in P8 heart at 7 days after injury compared with the sham group (Figure 4A). Compared with DMSO group, celecoxib treatment significantly reduced the levels of ANP, Myh7, and Acta1 in P8 heart at 7 days after injury (Figure 4A).

Next, we identified different pro-fibrotic gene expression in regenerative and non-regenerative neonatal mice at day 7 after injury. The mRNA expression levels of TGF-β2 and TGFBR1 were higher in P8 injured heart than in P3 injured heart at day 7, and celecoxib administration significantly reduced the mRNA levels

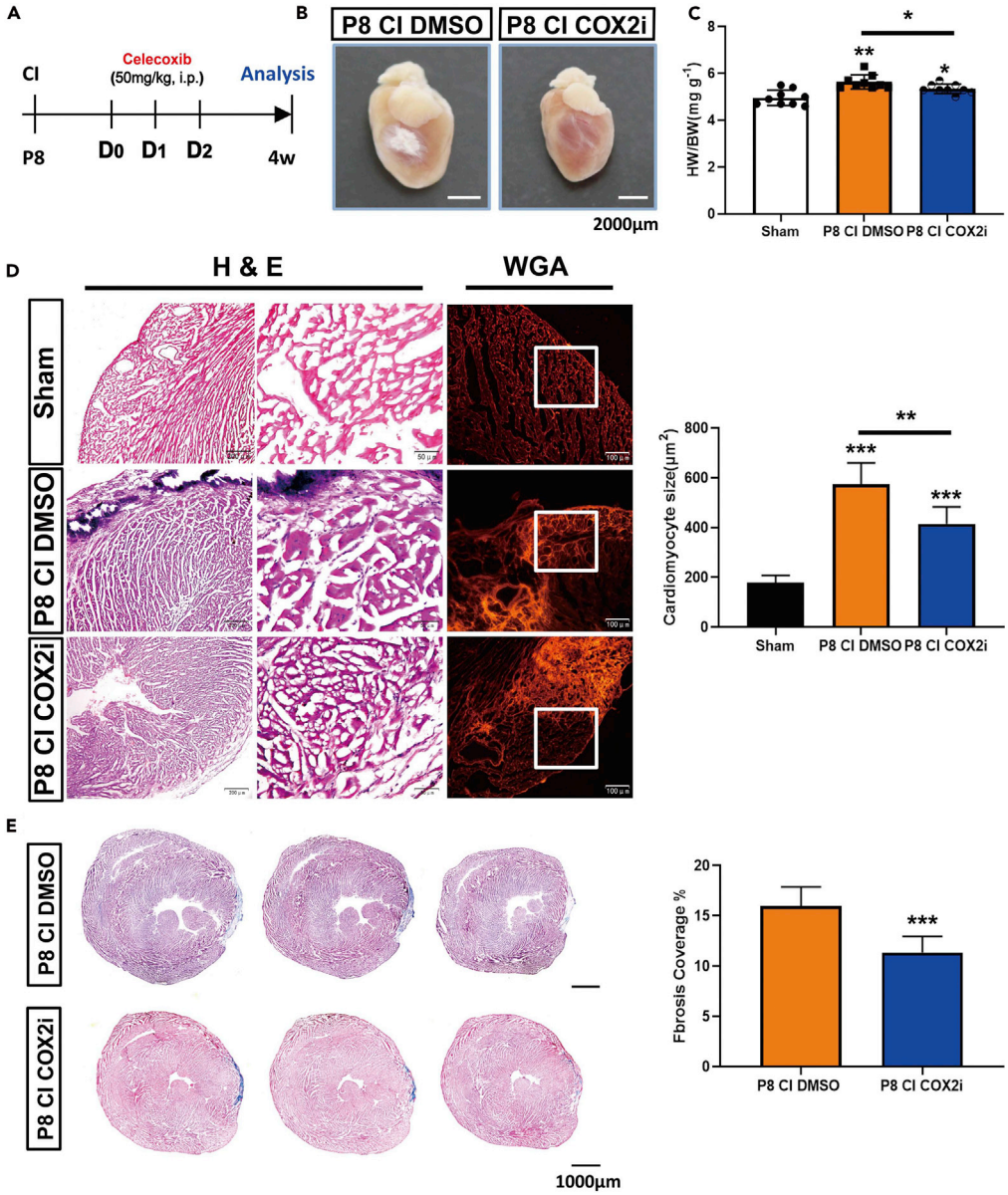

Figure 3. Celecoxib administration inhibited cardiac hypertrophy and fibrosis to repair injured neonatal heart in non-regenerative mice

(A) Experimental design of DMSO treated- and celecoxib-treated heart following CI and analysis for 4 weeks in (B–E).

(B) Neonatal ICR mice were intraperitoneally (i.p.) injected with DMSO and celecoxib at 50 mg/kg per mouse 0, 1, and 2 days after CI; scale bar, 2,000 μm.

(C and D) (C) Heart weight/body weight (mg/g) and (D) size of cardiomyocytes (μm^2) were measured by H&E and wheat germ agglutinin (WGA) staining in sham, DMSO treated-, and celecoxib-treated P8 mice at 4 weeks after injury; scale bars: 50 μm (400× objective), 100 μm (200× objective), and 200 μm (100× objective).

(E) Fibrosis coverage (%, 100 × scar perimeter/total perimeter) of heart tissue was measured using Masson's trichrome staining in DMSO treated- and celecoxib-treated P8 mice at 4 weeks after injury; scale bar, 1,000 μm. Data are representative of two independent experiments (n = 4–6 per group, mean ± SD. *p < 0.05, **p < 0.01, ***p < 0.001).

of TGF-β2 and TGFBR1 (Figure 4B). Meanwhile, the protein levels of TGF-β2 and TGF-β signaling-induced Snail were reduced after celecoxib administration at 7 days after injury (Figure 4C). These data demonstrated that celecoxib administration inhibited pro-fibrotic gene expression in non-regenerative mice at 7 days after injury, thereby suppressing cardiac hypertrophy and fibrosis at an early stage after injury.

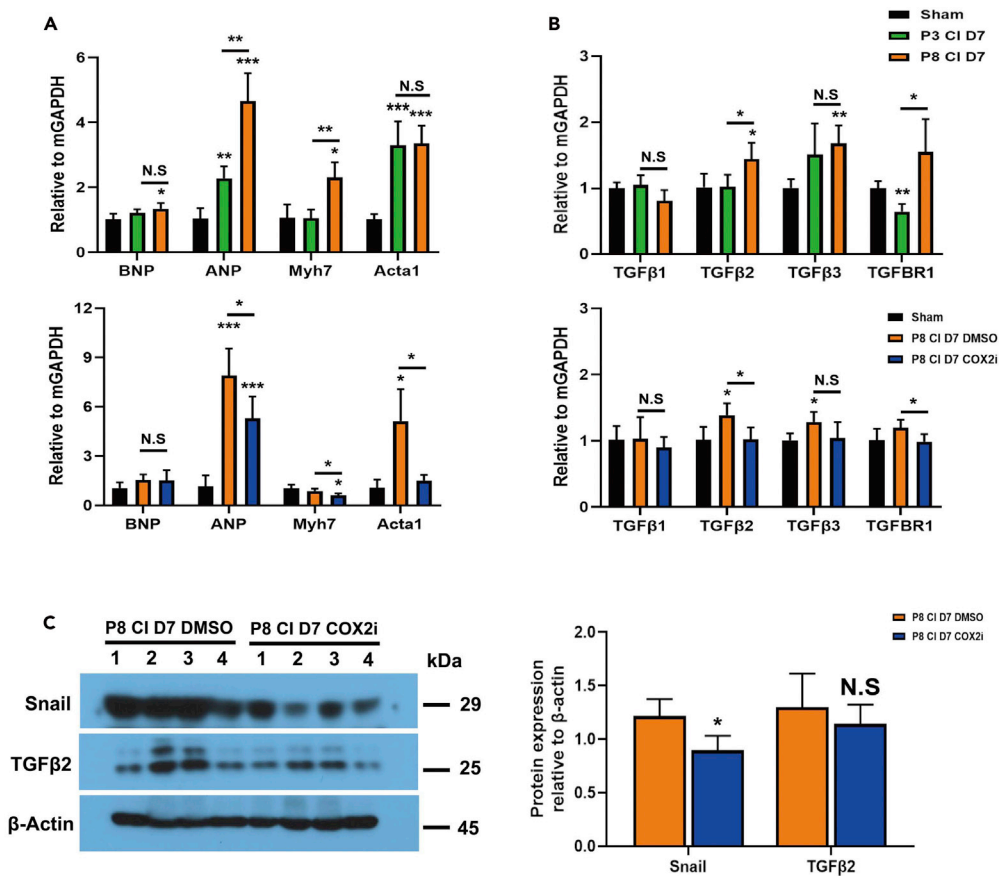

Figure 4. Celecoxib administration reduced cardiac hypertrophic and fibrotic gene expression as well as inflammatory-related gene expression in non-regenerative mice following injury

(A and B) (A) mRNA levels of hypertrophic genes and (B) pro-fibrotic genes were analyzed in sham, P3, P8, and DMSO-treated and celecoxib-treated P8 mice at 7 days after injury;

(C) Protein levels of pro-fibrotic genes and Snail in DMSO treated- and celecoxib-treated P8 mice were measured by western blot at 7 days after injury, respectively. Data are representative of two independent experiments (n = 5–6 per group, mean ± SD. *p < 0.05, **p < 0.01, ***p < 0.001).

Immune response plays a critical role in cardiac repair and regeneration (Lai et al., 2019; Wang et al., 2019a). The recent studies suggested that Ly6C+ monocyte subset was significantly increased within 24 h after neonatal heart injury, and macrophages were required for neonatal heart regeneration (Aurora et al., 2014; Wang et al., 2019b, 2020). Also, increasing studies illustrated that mRNA expression of MCP-1 was significantly increased at different time points after skin injury, and peaked MCP-1 expression was at 3 and 5 h after injury (Bai et al., 2008; Rezvan et al., 2020). In context of atherosclerotic lesions, mRNA expression of MCP-1 was significantly upregulated at 15 weeks after consecutive celecoxib treatment compared with the untreated group (Bea, 2003). Also, previous studies showed that PGE_2, a product of COX-2, would inhibit MCP-1 expression *in vivo* and *in vitro* (Largo et al., 2004; Schneider et al., 1999).

Thus, we performed real-time PCR and ELISA to demonstrate whether MCP-1 was induced at the early stage of injury in celecoxib treatment (Figure 5A). Our data showed that mRNA levels of MCP-1 significantly increased at D1, D3, and D7 in celecoxib-treated P8 CI mice compared with that of Sham and DMSO-treated P8 mice (Figure 5B). The protein expression levels of MCP-1 was significantly upregulated at 3 and 7 days in celecoxib-treated compared with DMSO-treated P8 CI mice, but no difference was present at 1 day after injury (Figure 5C). Our data suggested that celecoxib treatment would upregulate MCP-1 expression, which may recruit M1-like macrophages to repair injured heart at the early stage of injury. To evaluate the role of the anti-inflammatory agent celecoxib on the production of inflammatory stimuli after cardiac injury, we performed western blot to identify chemokine (MCP-1) and adhesion molecular genes (VCAM-I and ICAM-I) in the infarct/border zone

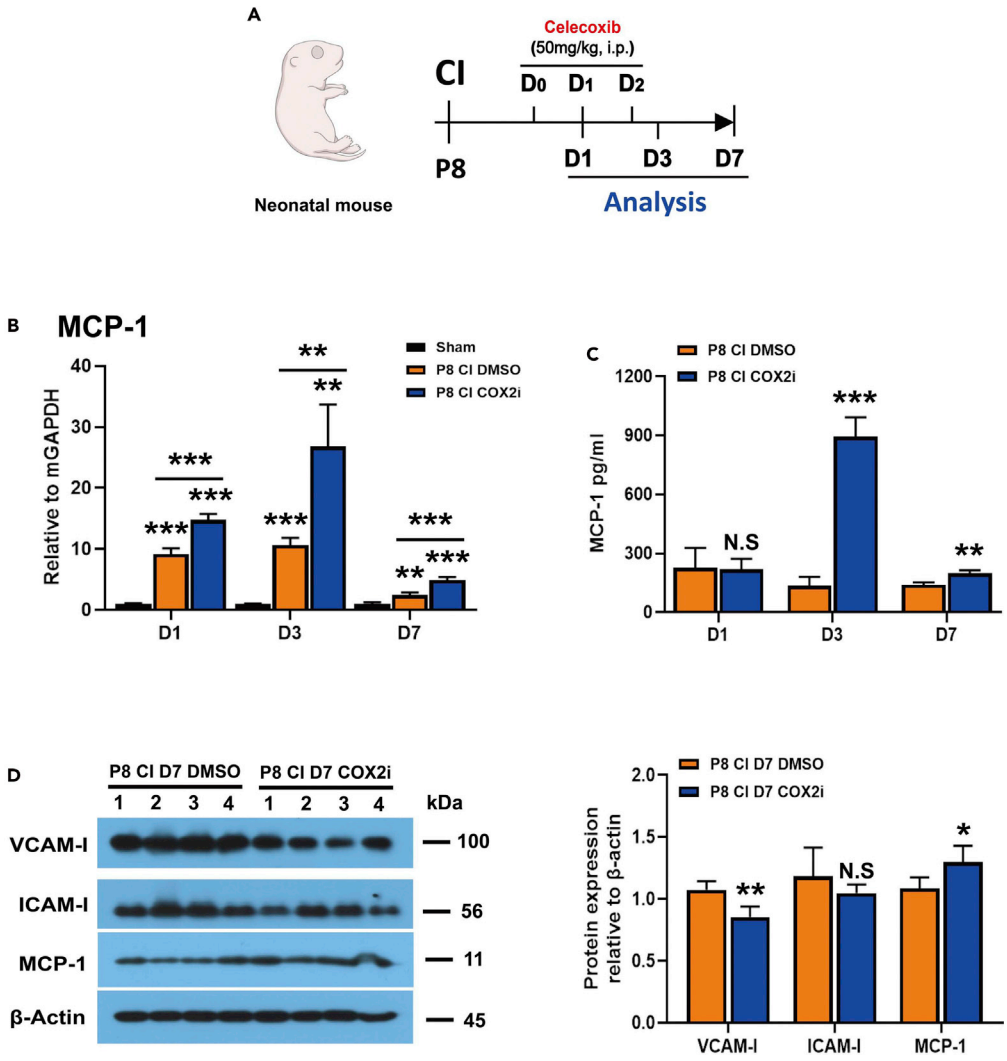

Figure 5. Celecoxib administration inhibited inflammatory-related gene expression in non-regenerative mice following injury

(A–D) (A) Experimental design of DMSO treated- and celecoxib-treated heart following CI and analysis for 1, 3, and 7 days in (B–D). mRNA levels (B) or protein levels (C) of MCP-1 were measured by real-time PCR or ELISA in both groups; protein levels of (D) chemokines and adhesion molecular genes were measured by western blot at 7 days after injury in DMSO treated- and celecoxib-treated P8 mice. Data are representative of two independent experiments (n = 5–6 per group, mean ± SD; *p < 0.05, **p < 0.01, ***p < 0.001).

at 7 days after injury. We found that the protein level of VCAM-I significantly reduced, whereas that of MCP-1 slightly increased in celecoxib-treated P8 heart at 7 days after CI (Figure 5D).

These data demonstrated that COX-2 inhibition reduced the expression of inflammatory cytokines and VCAM-I but upregulated MCP-1, which may contribute to the activation and migration of immune cell after cardiac injury.

Celecoxib modulates macrophages during cardiac hypertrophy and fibrosis

Various immune cells produce cytokines, chemokines, and other pathological stimuli; the previous studies showed that immune cell infiltration promoted cardiac hypertrophy and fibrosis (Frieler and Mortensen, 2015; Liu et al., 2019; Swirski and Nahrendorf, 2018). Accumulating evidence has shown that macrophages were required for heart regeneration and repair (Aurora et al., 2014; Simoes et al., 2020). In the present study, MCP-1 expression was significantly upregulated in the celecoxib-treated group at the early stage of injury, which may regulate macrophage migration (Figures 5B and 5C).

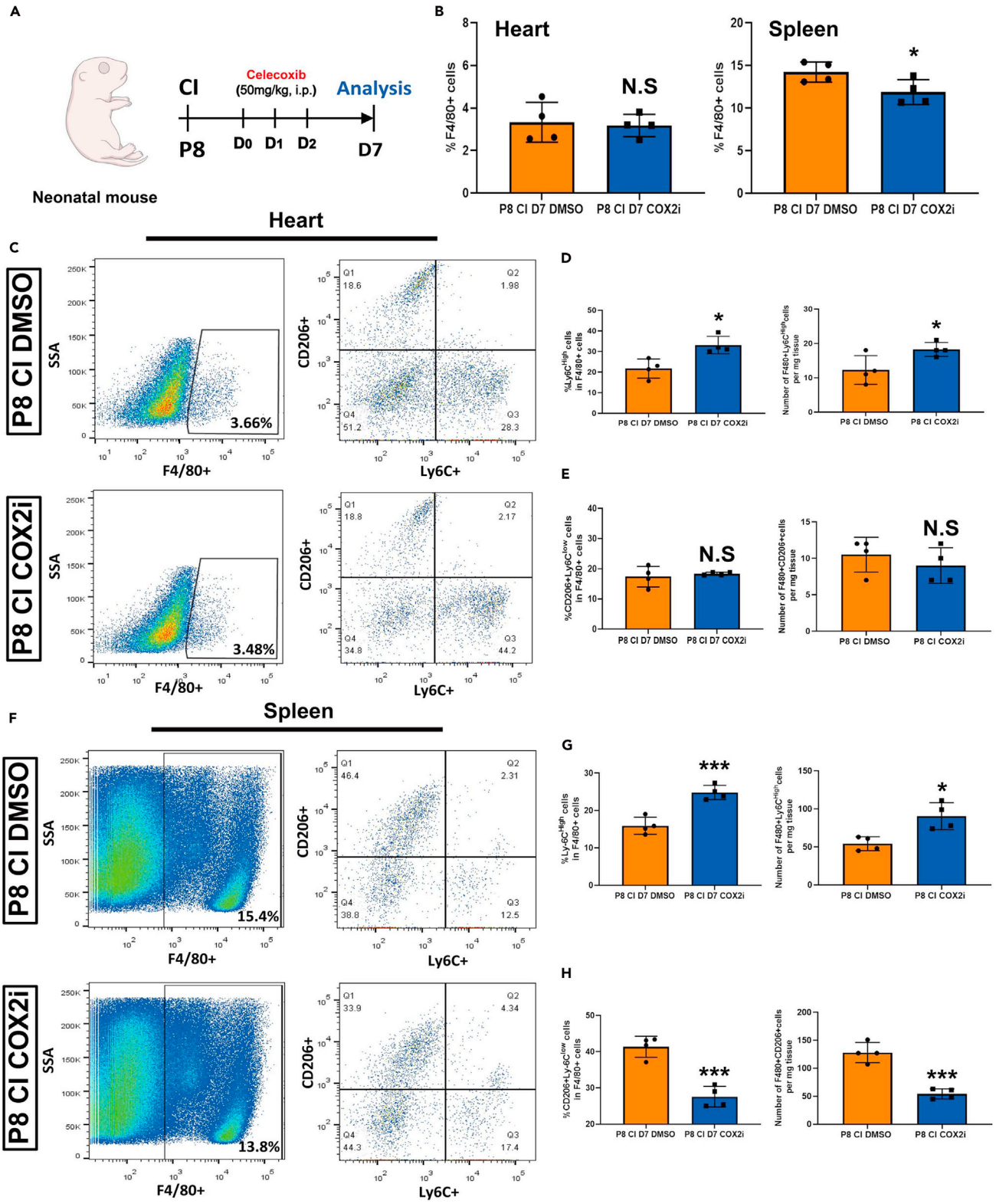

Figure 6. Celecoxib administration increased M1-like macrophage infiltration after injury

(A) Experimental design of DMSO treated- and celecoxib-treated P8 heart following CI and analysis for 7 days in (B–H).

(B–E) (B and C) Percentage of total F4/80+ macrophages of infarct/border zones was analyzed by flow cytometry at 7 days after injury; percentage and quantification of (D) M1-like macrophages (F480 + Ly6C ^{high} M1) and (E) M2-like macrophages (F480+ CD206+ Ly6C ^{low} M2).

Figure 6. *Continued*

(F–H) (F and G) Percentage and quantification of M1-like macrophages and (H) M2-like macrophages from the spleen were analyzed by flow cytometry in both groups the same as those in the heart. Data are representative of three independent experiments (n = 3–5 per group, mean ± SD, *p < 0.05, ***p < 0.001).

To investigate the role of macrophage in celecoxib administration during neonatal heart repair, we also identified M1-like (F4/80+ Ly6C+) and M2-like (F4/80+ CD206+ Ly6C-) macrophages among the total F4/80+ macrophages at 7 days after P8 heart injury (Figure 6A). We found no predominant difference in the percentage of all F4/80+ macrophages from the infarct/border zone of the celecoxib- and DMSO-treated groups, but the percentage of all F4/80+ macrophages from the spleen significantly reduced in the celecoxib-treated group compared with the DMSO-treated group (Figure 6B). Surprisingly, the percentage and number of M1-like macrophages from the infarct/border zone of the heart and spleen significantly increased in the celecoxib-administered group compared with the DMSO-treated group (Figures 6C, 6D, 6F, and 6G). Furthermore, the percentage and number of M2-like macrophages from all F4/80+ macrophages of the spleen considerably decreased in the celecoxib-treated group compared with the DMSO-treated group, whereas those of M2-like macrophages from the infarct/border zone of the heart showed no significant difference in both groups (Figures 6C, 6E, 6F, and 6H).

These observations demonstrated that COX-2 inhibition may regulate myocardial macrophages and polarize splenic macrophages to improve cardiac hypertrophy and fibrosis during the early process of neonatal heart repair.

Celecoxib treatment improves cardiac function through inhibition of inflammation after CI

To evaluate the role of the anti-inflammatory agent celecoxib on the production of inflammatory stimuli after cardiac injury, we performed real-time PCR to identify pro-inflammatory mediators in the infarct/border zone at 4 weeks after injury (primers listed in Table 1). In the production of pro-inflammatory cytokines, the mRNA levels of TNF-α, IFN-γ, IL-6, IL-1β, IL-17, and IL-21, especially those of IL-6 and IL-1β, were reduced after celecoxib administration (Figure 7A). Interestingly, the expression of the anti-inflammatory cytokine IL-10 significantly reduced in P8 heart when treated with celecoxib (Figure 7A). In addition, the mRNA levels of MCP-1, VCAM-I, and ICAM-I significantly decreased at 4 weeks after injury when treated with celecoxib (Figure 7B).

Consequently, we evaluated the role of celecoxib treatment in cardiac function at 4 weeks after injury. Interestingly, the end-diastolic volumes (EDVs), end-systolic volumes (ESVs), and intraventricular septal thickness at the end diastole (IVSd) significantly decreased in the celecoxib-treated group compared with the DMSO-treated group at 4 weeks after injury (Figures 7C and 7D). Moreover, the posterior wall thickness at the systole of left ventricle (LVPWs) increased after injury (Figure 7D). Internal diameters at the end diastole/systole (LVIDd/s), posterior wall thickness at the end diastole (LVPWd), intraventricular septal thickness at the end systole (IVSs), ejection fraction (EF%), and fractional shortening (FS%) showed no significant differences between the celecoxib-treated mice and the DMSO-treated mice at 4 weeks after injury (Figures 7C–7F). Thus, short time of celecoxib administration would improve cardiac function after injury.

DISCUSSION

Pathological cardiac hypertrophy is commonly induced by pathological stimuli and mechanical forces, resulting in cardiomyopathy death, and cardiac fibrosis. Accumulating evidence demonstrated that COX-2 is involved in cardiac hypertrophy and fibrosis (Chi et al., 2017; Li et al., 2014). Specific overexpression of COX-2 contributes to cardiac hypertrophy in mice, whereas COX-2 inhibition improves angiotensin- and aldosterone-induced hypertrophic response *in vitro* (Streicher et al., 2010; Wang et al., 2010). COX-2 expression triggers inflammatory response, cell apoptosis, and fibrosis after injury, which aggravate brain (Dehlaghi Jadid et al., 2019), renal (Fujihara et al., 2003), lung (Song et al., 2002), and skin (Romana-Souza et al., 2016) injuries. Overexpression of COX-2 is involved in vascular endothelial cell dysfunction and cardiac injury during inflammatory condition (Pang et al., 2016; Yin et al., 2017). The present study investigated whether or not selective COX-2 inhibition suppresses cardiac hypertrophy and fibrosis by mediating macrophages after injury or serves a regenerative function after injury in non-regenerative mice. We first demonstrated that hypertrophic response was only induced in non-regenerative mice compared with severe CI of regenerative mice. Although COX-2 expression was found in both groups after heart injury, the non-regenerative mice lost their regenerative capacity compared with the regenerative mice. In addition,

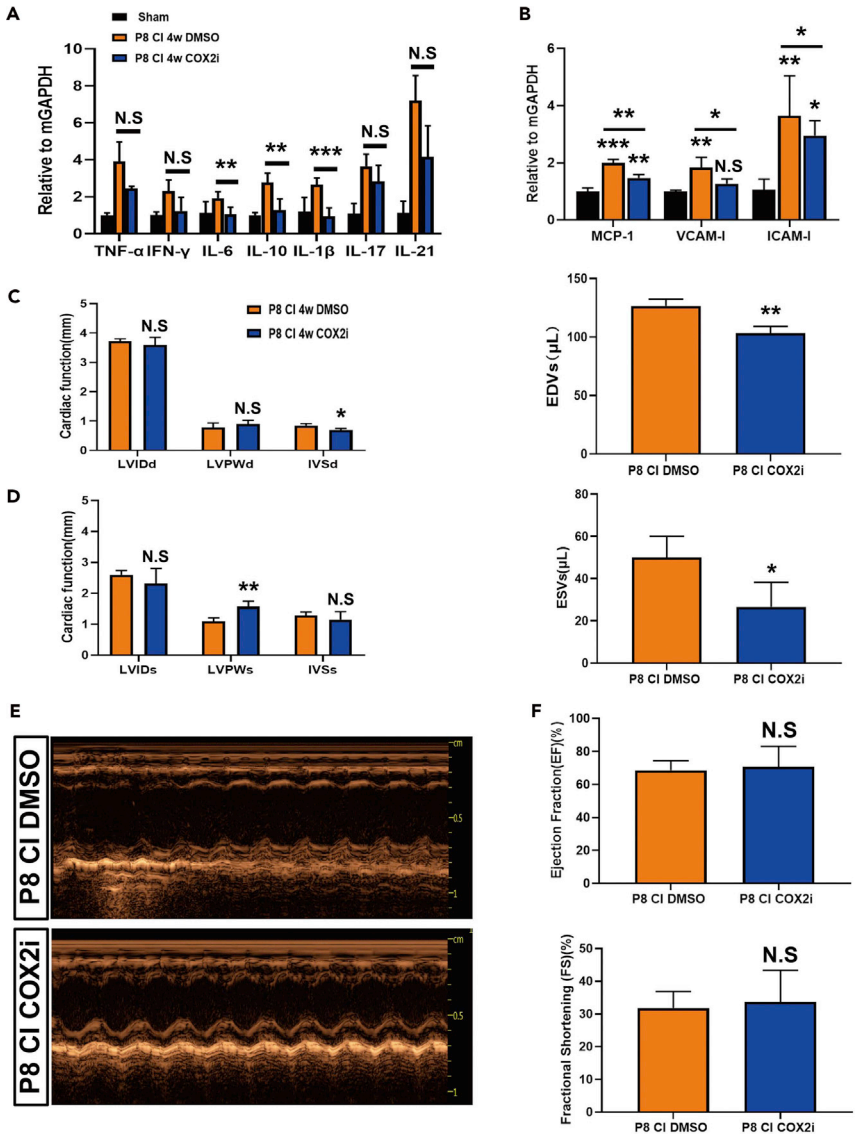

Figure 7. Celecoxib improved cardiac function by inhibiting inflammatory response after injury

(A and B) (A) The mRNA levels of cytokines and (B) chemokines as well as adhesion molecular genes were measured by real-time PCR at 4 weeks after injury in DMSO treated- and celecoxib-treated P8 mice.

(C–F) (C and D) Internal diameters (LVID), posterior wall thickness (LVPW), and intraventricular septal thickness (IVS) at the end diastole (C) or at the end systole (D) of the left ventricle and end-diastolic/systolic volume (EDVs and ESVs) were analyzed by a digital ultrasound system (E) at 4 weeks following cryoinjury. (F) Ejection fraction (EF%) and fractional shortening (FS%) were measured by a digital ultrasound system, the same as that in (E). Data are representative of mean ± SD (n = 5 per group, *p < 0.05, **p < 0.01, ***p < 0.001).

the expression levels of pro-inflammatory cytokines (IL-6 and IL-1β), adhesion molecule genes (ICAM-I), and pro-fibrotic gene expression (TGF-β2) were significantly upregulated in non-regenerative mice. This result demonstrates that upregulated COX-2 expression could be a central mediator in immune response during cardiac hypertrophy and fibrosis after injury.

Previous studies showed that selective COX-2 inhibitors exert a detrimental effect on cardiac vascular cells and heart after MI, contributing to reduced production of cardioprotective PGI_2 and increased infarct size and mortality in high-dose celecoxib administration (Camitta et al., 2001; Timmers et al., 2007). Recent

studies have demonstrated that selective COX-2 inhibitors with moderate-dose administration exert no detrimental effects on cardiovascular disease (Beales, 2020; Schjerning et al., 2020). Meanwhile, the infarct size of adult heart at the early stage of MI shows no significant changes in COX-2 knockout or inhibition with celecoxib compared with that in wild-type mice (Guo et al., 2000; Zhu et al., 2019). In a cardiac hypertrophy rat model, celecoxib inhibits inflammation and cardiac cell apoptosis after MI and subsequently improves pressure overload-induced cardiac hypertrophy in adult heart (Zhang et al., 2016). In neonatal CI model, we performed celecoxib treatment to non-regenerative mouse heart (P8) at the early stage of injury (D0, D1, and D2). Our data demonstrated that cardiac hypertrophy (HW/BW, and cardiomyocyte size) and fibrosis (fibrosis coverage [%]) significantly reduced at 4 weeks after injury in celecoxib administration. Meanwhile, hypertrophic (ANP, Myh7, and Acta1) and pro-fibrotic (TGF-β2 and TGFBR1) gene expression reduced in the treated group. These data suggest that celecoxib inhibited CI-induced cardiac hypertrophy and fibrosis in non-regenerative mice.

Given its capacity to promote cardiac structure, inflammatory response plays a central mediator in cardiac remodeling after injury (Frangogiannis, 2015; Nahrendorf et al., 2010). Recent studies have suggested that celecoxib inhibits the recruited cell number of CD4+T cells, F/480+ macrophages, and neutrophils at wound sites (Geesala et al., 2017; Wilgus et al., 2003). As for macrophage function, M1-like macrophages promote pro-inflammatory response at the early stage of wound healing after injury, contributing to clear dead cells and necrotic debris at wound sites. Consequently, M2-like macrophages play an anti-inflammatory role in the late stage of wound healing by releasing cytokines, chemokines, and pro-fibrotic growth factors, thereby regulating scar formation for tissue repair (Braga et al., 2015; Simoes et al., 2020). More interestingly, mounting studies reported that macrophages improved heart regeneration or repair in neonatal heart after injury, but not in adult injured heart (Aurora et al., 2014; Lavine et al., 2014). This means that macrophages-mediated cardiac repair has different functions in neonates and adults because of developmental and immunological difference (Li et al., 2020). Meanwhile, other groups performed transversal aortic constriction (TAC) to induce adult cardiac hypertrophy, and celecoxib administration improved pressure overload-induced hypertrophic response and inflammation in adult injury model as well (Jacobshagen et al., 2008; Zhang et al., 2016). However, the infarct size of adult heart at 24 h after MI showed no significant changes in COX-2 knockout or celecoxib treatment compared with that in wild-type mice (Guo et al., 2000; Zhu et al., 2019). The difference would demonstrate that neonatal CI model could be an ideal model to evaluate the effect of celecoxib on cardiac hypertrophy and fibrosis.

Also, accumulating studies showed that PGE_2 would inhibit MCP-1 expression *in vivo* and *in vitro* (Largo et al., 2004; Schneider et al., 1999). In the present study, MCP-1 expression was significantly upregulated after celecoxib treatment at the early stage of injury but downregulated at the later stage of injury, which may contribute to macrophage recruitment via CCL2/MCP-1 signaling. In addition, the recruited number or percentage of M1-like macrophages increased in the celecoxib-treated group compared with the DMSO-treated group in the infarct/border zone at 7 days after injury, whereas that of M2-like macrophages showed no significant difference in both groups. However, polarization of M2-to-M1-like macrophages was detected in the spleen after celecoxib administration. In line with a previous study (Jürgensen et al., 2019), emerging data suggested that M1-like ($F4/80^+Ly6c^+$) macrophages have a higher capacity of collagen and fibrin uptake for tissue repair after injury compared with M2-like macrophages and that no significant reduction of M2-like macrophages can be observed. Taken together, our data demonstrated that celecoxib can inhibit cardiac hypertrophy and fibrosis in non-regenerative mice by regulating M1-like macrophage infiltration. COX-2 is inducible by other pathological stimuli after injury; thus the regulatory mechanism of COX-2 should be further investigated in immune response-mediated cardiac hypertrophy and fibrosis.

Limitations of the study

CI-induced cardiac hypertrophy has been observed in neonatal mice, and CI was performed to successfully establish cardiac hypertrophy in ICR neonatal mice. CI was only performed on ICR neonatal mice. Different injury models and mouse strains should be considered in future studies.

Resource availability

Lead contact

Yanli, Zhao, Assistant Research Fellow, Department of Medical Laboratory, Shenzhen Longhua District Central Hospital, Affiliated Central Hospital of Shenzhen Longhua District, Guangdong Medical University, Shenzhen, China, Email: yanlizhao2015@126.com.

Material availability

Requests for materials and reagents should be address to the lead contact, Yanli, Zhao, yanlizhao2015@126.com.

Data and code availability

Raw count data of RNA-seq were retrieved from the Gene Expression Omnibus (GEO) database (https://www.ncbi.nlm.nih.gov/geo) under the accession no. GSE123868 (Wang et al., 2019b).

METHODS

All methods can be found in the accompanying Transparent Methods supplemental file.

SUPPLEMENTAL INFORMATION

Supplemental information can be found online at https://doi.org/10.1016/j.isci.2021.102233.

ACKNOWLEDGMENTS

We thank Mr. Dexin Yang and Mr. Wenkai Zhang for technical help in blindly taking animal samples. This work was supported by Shenzhen Longhua District key laboratory of infection and immunity project (China).

AUTHOR CONTRIBUTIONS

Y.Z. performed experiments, Q.Z. performed bioinformatics analysis, Y.Z., and Q.Z. analyzed the data, H.G., M.C., H.W., and C.Z. contributed to reagents and machinery support, Y.Z., R.C., and C.Z. interpreted the experimental data, Y.Z., and C.Z. designed and wrote the manuscript.

DECLARATION OF INTERESTS

The authors have no conflict of interest.

Received: October 18, 2020
Revised: January 13, 2021
Accepted: February 22, 2021
Published: March 19, 2021

REFERENCES

Al-Rashed, F., Calay, D., Lang, M., Thornton, C.C., Bauer, A., Kiprianos, A., Haskard, D.O., Seneviratne, A., Boyle, J.J., Schonthal, A.H., et al. (2018). Celecoxib exerts protective effects in the vascular endothelium via COX-2-independent activation of AMPK-CREB-Nrf2 signalling. Sci. Rep. *8*, 6271.

Aurora, A.B., Porrello, E.R., Tan, W., Mahmoud, A.I., Hill, J.A., Bassel-Duby, R., Sadek, H.A., and Olson, E.N. (2014). Macrophages are required for neonatal heart regeneration. J. Clin. Invest. *124*, 1382–1392.

Bai, R., Wan, L., and Shi, M. (2008). The time-dependent expressions of IL-1beta, COX-2, MCP-1 mRNA in skin wounds of rabbits. Forensic Sci. Int. *175*, 193–197.

Bea, F. (2003). Chronic inhibition of cyclooxygenase-2 does not alter plaque composition in a mouse model of advanced unstable atherosclerosis. Cardiovasc. Res. *60*, 198–204.

Beales, I.L.P. (2020). Selective COX-2 inhibitors are safe and effective. BMJ *368*, m311.

Braga, T.T., Agudelo, J.S., and Camara, N.O. (2015). Macrophages during the fibrotic process: M2 as friend and foe. Front. Immunol. *6*, 602.

Camitta, M.G., Gabel, S.A., Chulada, P., Bradbury, J.A., Langenbach, R., Zeldin, D.C., and Murphy, E. (2001). Cyclooxygenase-1 and -2 knockout mice demonstrate increased cardiac ischemia/reperfusion injury but are protected by acute preconditioning. Circulation *104*, 2453–2458.

Chenevard, R., Hurlimann, D., Bechir, M., Enseleit, F., Spieker, L., Hermann, M., Riesen, W., Gay, S., Gay, R.E., Neidhart, M., et al. (2003). Selective COX-2 inhibition improves endothelial function in coronary artery disease. Circulation *107*, 405–409.

Chi, Y.C., Shi, C.L., Zhou, M., Liu, Y., Zhang, G., and Hou, S.A. (2017). Selective cyclooxygenase-2 inhibitor NS-398 attenuates myocardial fibrosis in mice after myocardial infarction via Snail signaling pathway. Eur. Rev. Med. Pharmacol. Sci. *21*, 5805–5812.

Cui, M., Wang, Z., Chen, K., Shah, A.M., Tan, W., Duan, L., Sanchez-Ortiz, E., Li, H., Xu, L., Liu, N., et al. (2020). Dynamic transcriptional responses to injury of regenerative and non-regenerative cardiomyocytes revealed by single-nucleus RNA sequencing. Dev. Cell *53*, 102–116 e108.

Dehlaghi Jadid, K., Davidsson, J., Lidin, E., Hanell, A., Angeria, M., Mathiesen, T., Risling, M., and Gunther, M. (2019). COX-2 inhibition by diclofenac is associated with decreased apoptosis and lesion area after experimental focal penetrating traumatic brain injury in rats. Front. Neurol. *10*, 811.

Ding, J., Lei, L., Liu, S., Zhang, Y., Yu, Z., Su, Y., and Ma, X. (2019). Macrophages are necessary for skin regeneration during tissue expansion. J. Transl. Med. *17*, 36.

Epelman, S., Liu, P.P., and Mann, D.L. (2015). Role of innate and adaptive immune mechanisms in cardiac injury and repair. Nat. Rev. Immunol. *15*, 117–129.

Feniman De Stefano, G.M.M., Zanati-Basan, S.G., De Stefano, L.M., Silva, V.R.O.e., Xavier, P.S., Barretti, P., da Silva Franco, R.J., Caramori, J.C.T., and Martin, L.C. (2016). Aldosterone is associated with left ventricular hypertrophy in hemodialysis patients. Ther. Adv. Cardiovasc. Dis. *10*, 304–313.

Frangogiannis, N.G. (2015). Inflammation in cardiac injury, repair and regeneration. Curr. Opin. Cardiol. *30*, 240–245.

Frieler, R.A., and Mortensen, R.M. (2015). Immune cell and other noncardiomyocyte regulation of cardiac hypertrophy and remodeling. Circulation *131*, 1019–1030.

Fujihara, C.K., Antunes, G.R., Mattar, A.L., Andreoli, N., Malheiros, D.M., Noronha, I.L., and Zatz, R. (2003). Cyclooxygenase-2 (COX-2) inhibition limits abnormal COX-2 expression and progressive injury in the remnant kidney. Kidney Int. *64*, 2172–2181.

Geesala, R., Dhoke, N.R., and Das, A. (2017). Cox-2 inhibition potentiates mouse bone marrow stem cell engraftment and differentiation-mediated wound repair. Cytotherapy *19*, 756–770.

Guo, Y., Bao, W., Wu, W.J., Shinmura, K., Tang, X.L., and Bolli, R. (2000). Evidence for an essential role of cyclooxygenase-2 as a mediator of the late phase of ischemic preconditioning in mice. Basic Res. Cardiol. *95*, 479–484.

Homma, T., Kinugawa, S., Takahashi, M., Sobirin, M.A., Saito, A., Fukushima, A., Suga, T., Takada, S., Kadoguchi, T., Masaki, Y., et al. (2013). Activation of invariant natural killer T cells by alpha-galactosylceramide ameliorates myocardial ischemia/reperfusion injury in mice. J. Mol. Cell Cardiol. *62*, 179–188.

Huang, H., Chen, J., Peng, L., Yao, Y., Deng, D., Zhang, Y., Liu, Y., Wang, H., Li, Z., Bi, Y., et al. (2019). Transgenic expression of cyclooxygenase-2 in pancreatic acinar cells induces chronic pancreatitis. Am. J. Physiol. Gastrointest. Liver Physiol. *316*, G179–G186.

Jacobshagen, C., Gruber, M., Teucher, N., Schmidt, A.G., Unsold, B.W., Toischer, K., Nguyen, V.P., Maier, L.S., Kogler, H., and Hasenfuss, G. (2008). Celecoxib modulates hypertrophic signalling and prevents load-induced cardiac dysfunction. Eur. J. Heart Fail *10*, 334–342.

Jürgensen, H.J., Silva, L.M., Krigslund, O., van Putten, S., Madsen, D.H., Behrendt, N., Engelholm, L.H., and Bugge, T.H. (2019). CCL2/MCP-1 signaling drives extracellular matrix turnover by diverse macrophage subsets. Matrix Biol. Plus *1*, 100003.

Kaushik, K., and Das, A. (2019). Cycloxygenase-2 inhibition potentiates trans-differentiation of Wharton's jelly-mesenchymal stromal cells into endothelial cells: transplantation enhances neovascularization-mediated wound repair. Cytotherapy *21*, 260–273.

Konfino, T., Landa, N., Ben-Mordechai, T., and Leor, J. (2015). The type of injury dictates the mode of repair in neonatal and adult heart. J. Am. Heart Assoc. *4*, e001320.

Kuwahara, F., Kai, H., Tokuda, K., Kai, M., Takeshita, A., Egashira, K., and Imaizumi, T. (2002). Transforming growth factor-beta function blocking prevents myocardial fibrosis and diastolic dysfunction in pressure-overloaded rats. Circulation *106*, 130–135.

Kvakan, H., Kleinewietfeld, M., Qadri, F., Park, J.K., Fischer, R., Schwarz, I., Rahn, H.P., Plehm, R., Wellner, M., Elitok, S., et al. (2009). Regulatory T cells ameliorate angiotensin II-induced cardiac damage. Circulation *119*, 2904–2912.

Lai, S.L., Marin-Juez, R., and Stainier, D.Y.R. (2019). Immune responses in cardiac repair and regeneration: a comparative point of view. Cell. Mol. Life Sci. *76*, 1365–1380.

LaPointe, M.C., Mendez, M., Leung, A., Tao, Z., and Yang, X.P. (2004). Inhibition of cyclooxygenase-2 improves cardiac function after myocardial infarction in the mouse. Am. J. Physiol. Heart Circ. Physiol. *286*, H1416–H1424.

Largo, R., Diez-Ortego, I., Sanchez-Pernaute, O., Lopez-Armada, M.J., Alvarez-Soria, M.A., Egido, J., and Herrero-Beaumont, G. (2004). EP2/EP4 signalling inhibits monocyte chemoattractant protein-1 production induced by interleukin 1beta in synovial fibroblasts. Ann. Rheum. Dis. *63*, 1197–1204.

Lavine, K.J., Epelman, S., Uchida, K., Weber, K.J., Nichols, C.G., Schilling, J.D., Ornitz, D.M., Randolph, G.J., and Mann, D.L. (2014). Distinct macrophage lineages contribute to disparate patterns of cardiac recovery and remodeling in the neonatal and adult heart. Proc. Natl. Acad. Sci. U S A *111*, 16029–16034.

Li, H., Gao, S., Ye, J., Feng, X., Cai, Y., Liu, Z., Lu, J., Li, Q., Huang, X., Chen, S., et al. (2014). COX-2 is involved in ET-1-induced hypertrophy of neonatal rat cardiomyocytes: role of NFATc3. Mol. Cell. Endocrinol. *382*, 998–1006.

Li, Y., Li, H., Pei, J., Hu, S., and Nie, Y. (2020). Transplantation of murine neonatal cardiac macrophage improves adult cardiac repair. Cell. Mol. Immunol. *18*, 492–494.

Li, Y., Soendergaard, C., Bergenheim, F.H., Aronoff, D.M., Milne, G., Riis, L.B., Seidelin, J.B., Jensen, K.B., and Nielsen, O.H. (2018). COX-2-PGE2 signaling impairs intestinal epithelial regeneration and associates with TNF inhibitor responsiveness in ulcerative colitis. EBioMedicine *36*, 497–507.

Liu, Y., Lu, H., Zhang, C., Hu, J., and Xu, D. (2019). Recent advances in understanding the roles of T cells in pressure overload-induced cardiac hypertrophy and remodeling. J. Mol. Cell. Cardiol. *129*, 293–302.

Ma, N., Szabolcs, M.J., Sun, J., Albala, A., Sciacca, R.R., Zhong, M., Edwards, N., and Cannon, P.J. (2002). The effect of selective inhibition of cyclooxygenase (COX)-2 on acute cardiac allograft rejection. Transplantation *74*, 1528–1534.

Ma, Y., Su, K.N., Pfau, D., Rao, V.S., Wu, X., Hu, X., Leng, L., Du, X., Piecychna, M., and Bedi, K. (2019). Cardiomyocyte d-dopachrome tautomerase protects against heart failure. JCI Insight *4*, e128900.

Mahdavian Delavary, B., van der Veer, W.M., van Egmond, M., Niessen, F.B., and Beelen, R.H. (2011). Macrophages in skin injury and repair. Immunobiology *216*, 753–762.

Mahmoud, A.I., Porrello, E.R., Kimura, W., Olson, E.N., and Sadek, H.A. (2014). Surgical models for cardiac regeneration in neonatal mice. Nat. Protoc. *9*, 305–311.

Manabe, I., Shindo, T., and Nagai, R. (2002). Gene expression in fibroblasts and fibrosis: involvement in cardiac hypertrophy. Circ. Res. *91*, 1103–1113.

Mantovani, A., Sica, A., Sozzani, S., Allavena, P., Vecchi, A., and Locati, M. (2004). The chemokine system in diverse forms of macrophage activation and polarization. Trends Immunol. *25*, 677–686.

Nahrendorf, M., Pittet, M.J., and Swirski, F.K. (2010). Monocytes: protagonists of infarct inflammation and repair after myocardial infarction. Circulation *121*, 2437–2445.

Nakamura, M., and Sadoshima, J. (2018). Mechanisms of physiological and pathological cardiac hypertrophy. Nat. Rev. Cardiol. *15*, 387–407.

Nissen, S.E., Yeomans, N.D., Solomon, D.H., Luscher, T.F., Libby, P., Husni, M.E., Graham, D.Y., Borer, J.S., Wisniewski, L.M., Wolski, K.E., et al. (2016). Cardiovascular safety of celecoxib, naproxen, or ibuprofen for arthritis. N. Engl. J. Med. *375*, 2519–2529.

Pang, L., Cai, Y., Tang, E.H., Yan, D., Kosuru, R., Li, H., Irwin, M.G., Ma, H., and Xia, Z. (2016). Cox-2 inhibition protects against hypoxia/reoxygenation-induced cardiomyocyte apoptosis via akt-dependent enhancement of iNOS expression. Oxid. Med. Cell. Longev. *2016*, 3453059.

Polizzotti, B.D., Ganapathy, B., Haubner, B.J., Penninger, J.M., and Kuhn, B. (2016). A cryoinjury model in neonatal mice for cardiac translational and regeneration research. Nat. Protoc. *11*, 542–552.

Polizzotti, B.D., Ganapathy, B., Walsh, S., Choudhury, S., Ammanamanchi, N., Bennett, D.G., dos Remedios, C.G., Haubner, B.J., Penninger, J.M., and Kuhn, B. (2015). Neuregulin stimulation of cardiomyocyte regeneration in mice and human myocardium reveals a therapeutic window. Sci. Transl. Med. *7*, 281ra245.

Porrello, E.R., Mahmoud, A.I., Simpson, E., Hill, J.A., Richardson, J.A., Olson, E.N., and Sadek, H.A. (2011). Transient regenerative potential of the neonatal mouse heart. Science *331*, 1078–1080.

Rezvan, M., Meknatkhah, S., Hassannejad, Z., Sharif-Alhoseini, M., Zadegan, S.A., Shokraneh, F., Vaccaro, A.R., Lu, Y., and Rahimi-Movaghar, V. (2020). Time-dependent microglia and macrophages response after traumatic spinal cord injury in rat: a systematic review. Injury *51*, 2390–2401.

Robertson, R.P. (2017). The COX-2/PGE2/EP3/Gi/o/cAMP/GSIS pathway in the islet: the beat Goes on. Diabetes *66*, 1464–1466.

Romana-Souza, B., Santos, J.S., Bandeira, L.G., and Monte-Alto-Costa, A. (2016). Selective inhibition of COX-2 improves cutaneous wound healing of pressure ulcers in mice through reduction of iNOS expression. Life Sci. *153*, 82–92.

Rosenkranz, S., Flesch, M., Amann, K., Haeuseler, C., Kilter, H., Seeland, U., Schluter, K.D., and Bohm, M. (2002). Alterations of beta-adrenergic signaling and cardiac hypertrophy in transgenic

mice overexpressing TGF-beta(1). Am. J. Physiol. Heart Circ. Physiol. *283*, H1253–H1262.

Rumzhum, N.N., and Ammit, A.J. (2016). Cyclooxygenase 2: its regulation, role and impact in airway inflammation. Clin. Exp. Allergy *46*, 397–410.

Sakata, Y., Chancey, A.L., Divakaran, V.G., Sekiguchi, K., Sivasubramanian, N., and Mann, D.L. (2008). Transforming growth factor-beta receptor antagonism attenuates myocardial fibrosis in mice with cardiac-restricted overexpression of tumor necrosis factor. Basic Res. Cardiol. *103*, 60–68.

Schjerning, A.M., McGettigan, P., and Gislason, G. (2020). Cardiovascular effects and safety of (non-aspirin) NSAIDs. Nat. Rev. Cardiol. *17*, 574–584.

Schneider, A., Harendza, S., Zahner, G., Jocks, T., Wenzel, U., Wolf, G., Thaiss, F., Helmchen, U., and Stahl, R.A. (1999). Cyclooxygenase metabolites mediate glomerular monocyte chemoattractant protein-1 formation and monocyte recruitment in experimental glomerulonephritis. Kidney Int. *55*, 430–441.

Simoes, F.C., Cahill, T.J., Kenyon, A., Gavriouchkina, D., Vieira, J.M., Sun, X., Pezzolla, D., Ravaud, C., Masmanian, E., Weinberger, M., et al. (2020). Macrophages directly contribute collagen to scar formation during zebrafish heart regeneration and mouse heart repair. Nat. Commun. *11*, 600.

Slomski, A. (2016). Celecoxib similar to 2 NSAIDs for cardiovascular safety. JAMA *316*, 2589.

Sobirin, M.A., Kinugawa, S., Takahashi, M., Fukushima, A., Homma, T., Ono, T., Hirabayashi, K., Suga, T., Azalia, P., Takada, S., et al. (2012). Activation of natural killer T cells ameliorates postinfarct cardiac remodeling and failure in mice. Circ. Res. *111*, 1037–1047.

Song, A.M., Bhagat, L., Singh, V.P., Van Acker, G.G., Steer, M.L., and Saluja, A.K. (2002). Inhibition of cyclooxygenase-2 ameliorates the severity of pancreatitis and associated lung injury. Am. J. Physiol. Gastrointest. Liver Physiol. *283*, G1166–G1174.

Steffel, J., Hermann, M., Greutert, H., Gay, S., Luscher, T.F., Ruschitzka, F., and Tanner, F.C. (2005). Celecoxib decreases endothelial tissue factor expression through inhibition of c-Jun terminal NH2 kinase phosphorylation. Circulation *111*, 1685–1689.

Streicher, J.M., Kamei, K., Ishikawa, T.O., Herschman, H., and Wang, Y. (2010). Compensatory hypertrophy induced by ventricular cardiomyocyte-specific COX-2 expression in mice. J. Mol. Cell. Cardiol. *49*, 88–94.

Swirski, F.K., and Nahrendorf, M. (2018). Cardioimmunology: the immune system in cardiac homeostasis and disease. Nat. Rev. Immunol. *18*, 733–744.

Timmers, L., Sluijter, J.P., Verlaan, C.W., Steendijk, P., Cramer, M.J., Emons, M., Strijder, C., Grundeman, P.F., Sze, S.K., Hua, L., et al. (2007). Cyclooxygenase-2 inhibition increases mortality, enhances left ventricular remodeling, and impairs systolic function after myocardial infarction in the pig. Circulation *115*, 326–332.

Wang, B.H., Bertucci, M.C., Ma, J.Y., Adrahtas, A., Cheung, R.Y., and Krum, H. (2010). Celecoxib, but not rofecoxib or naproxen, attenuates cardiac hypertrophy and fibrosis induced in vitro by angiotensin and aldosterone. Clin. Exp. Pharmacol. Physiol. *37*, 912–918.

Wang, Y., Dembowsky, K., Chevalier, E., Stuve, P., Korf-Klingebiel, M., Lochner, M., Napp, L.C., Frank, H., Brinkmann, E., Kanwischer, A., et al. (2019a). C-X-C Motif chemokine receptor 4 blockade promotes tissue repair after myocardial infarction by enhancing regulatory T cell mobilization and immune-regulatory function. Circulation *139*, 1798–1812.

Wang, Z., Cui, M., Shah, A.M., Tan, W., Liu, N., Bassel-Duby, R., and Olson, E.N. (2020). Cell-type-Specific gene regulatory networks underlying murine neonatal heart regeneration at single-cell resolution. Cell Rep. *33*, 108472.

Wang, Z., Cui, M., Shah, A.M., Ye, W., Tan, W., Min, Y.L., Botten, G.A., Shelton, J.M., Liu, N., Bassel-Duby, R., et al. (2019b). Mechanistic basis of neonatal heart regeneration revealed by transcriptome and histone modification profiling. Proc. Natl. Acad. Sci. U S A *116*, 18455–18465.

Wilgus, T.A., Bergdall, V.K., Tober, K.L., Hill, K.J., Mitra, S., Flavahan, N.A., and Oberyszyn, T.M. (2004). The impact of cyclooxygenase-2 mediated inflammation on scarless fetal wound healing. Am. J. Pathol. *165*, 753–761.

Wilgus, T.A., Vodovotz, Y., Vittadini, E., Clubbs, E.A., and Oberyszyn, T.M. (2003). Reduction of scar formation in full-thickness wounds with topical celecoxib treatment. Wound Repair Regen. *11*, 25–34.

Wong, W.T., Tian, X.Y., and Huang, Y. (2013). Endothelial dysfunction in diabetes and hypertension: cross talk in RAS, BMP4, and ROS-dependent COX-2-derived prostanoids. J. Cardiovasc. Pharmacol. *61*, 204–214.

Wu, R., Laplante, M.A., and de Champlain, J. (2005). Cyclooxygenase-2 inhibitors attenuate angiotensin II-induced oxidative stress, hypertension, and cardiac hypertrophy in rats. Hypertension *45*, 1139–1144.

Wynn, T.A., and Vannella, K.M. (2016). Macrophages in tissue repair, regeneration, and fibrosis. Immunity *44*, 450–462.

Xia, H., Li, X., Gao, W., Fu, X., Fang, R.H., Zhang, L., and Zhang, K. (2018). Tissue repair and regeneration with endogenous stem cells. Nat. Rev. Mater. *3*, 174–193.

Yang, X., Ma, N., Szabolcs, M.J., Zhong, J., Athan, E., Sciacca, R.R., Michler, R.E., Anderson, G.D., Wiese, J.F., Leahy, K.M., et al. (2000). Upregulation of COX-2 during cardiac allograft rejection. Circulation *101*, 430–438.

Yin, J., Xia, W., Li, Y., Guo, C., Zhang, Y., Huang, S., Jia, Z., and Zhang, A. (2017). COX-2 mediates PM2.5-induced apoptosis and inflammation in vascular endothelial cells. Am. J. Transl. Res. *9*, 3967–3976.

Yu, W., Huang, X., Tian, X., Zhang, H., He, L., Wang, Y., Nie, Y., Hu, S., Lin, Z., Zhou, B., et al. (2016). GATA4 regulates Fgf16 to promote heart repair after injury. Development *143*, 936–949.

Zacchigna, S., Martinelli, V., Moimas, S., Colliva, A., Anzini, M., Nordio, A., Costa, A., Rehman, M., Vodret, S., Pierro, C., et al. (2018). Paracrine effect of regulatory T cells promotes cardiomyocyte proliferation during pregnancy and after myocardial infarction. Nat. Commun. *9*, 2432.

Zhang, C., Wang, F., Zhang, Y., Kang, Y., Wang, H., Si, M., Su, L., Xin, X., Xue, F., Hao, F., et al. (2016). Celecoxib prevents pressure overload-induced cardiac hypertrophy and dysfunction by inhibiting inflammation, apoptosis and oxidative stress. J. Cell. Mol. Med. *20*, 116–127.

Zhu, L., Xu, C., Huo, X., Hao, H., Wan, Q., Chen, H., Zhang, X., Breyer, R.M., Huang, Y., Cao, X., et al. (2019). The cyclooxygenase-1/mPGES-1/endothelial prostaglandin EP4 receptor pathway constrains myocardial ischemia-reperfusion injury. Nat. Commun. *10*, 1888.

iScience, Volume *24*

Supplemental information

Celecoxib alleviates pathological cardiac hypertrophy and fibrosis via M1-like macrophage infiltration in neonatal mice

Yanli Zhao, Qi Zheng, Hanchao Gao, Mengtao Cao, Huiyun Wang, Rong Chang, and Changchun Zeng

Figure S1

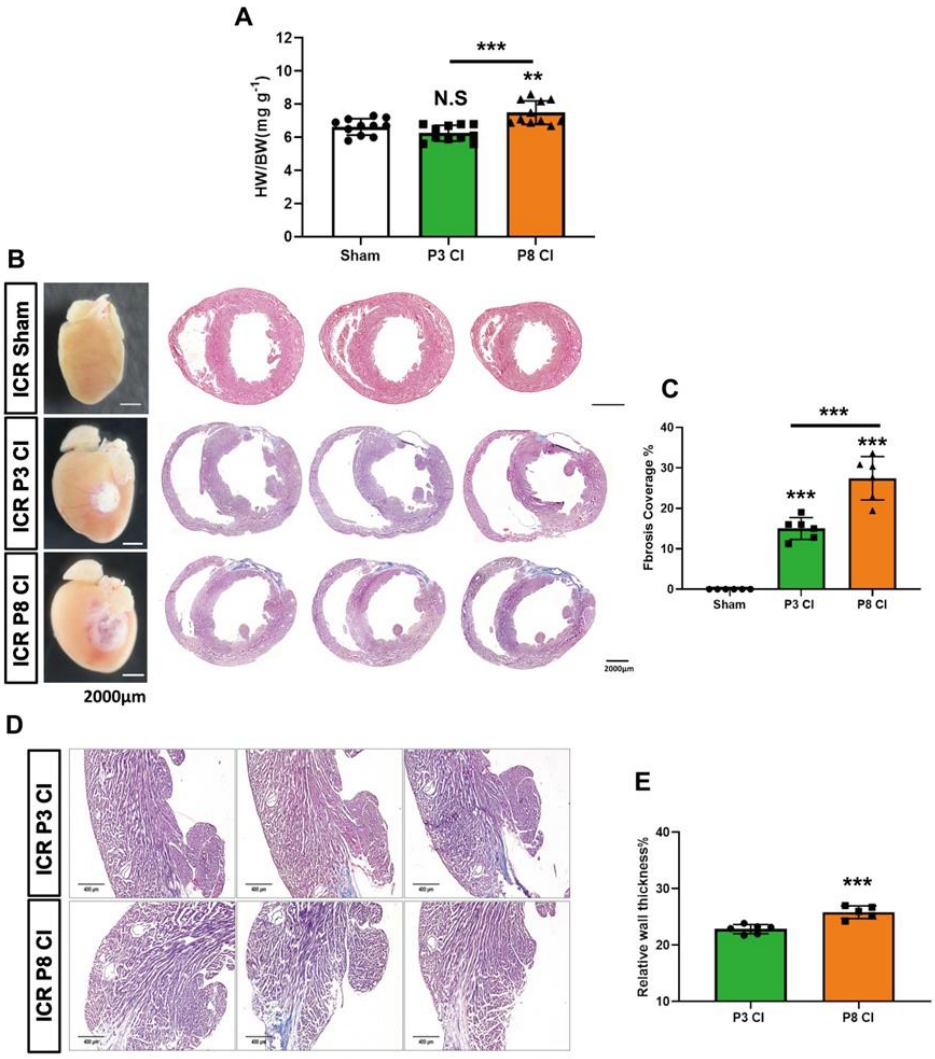

Fig S1: Cardiac hypertrophy and fibrosis were induced with severe cryoinjury in non-regenerative mice (P8) following CI, Related to Figure 1

(A) Heart weight/body weight (HW/BW, mg/g) in sham, regenerating mice (P3, at postnatal day 3), and non-regenerating mice (P8) at 4 weeks after injury（Copper wire area: 2 mm^2， ICR mother mice: 6-8 weeks）; **(B)** Heart tissue of P3 or P8 after injury was stained with Masson's trichrome, scale bar = 2000 μm; **(C)** Quantification of fibrosis coverage (%) in P3 and P8 left ventricle at 4 weeks following CI; **(D)** Masson Trichrome staining showing infarcted/border zone of P3 and P8 after injury, scale bar = 400μm; **(E)** Quantification of relative wall thickness (%) in P3 and P8 left ventricle at 4 weeks following CI, the formula of relative wall thickness(%): 100 x length of adjunctive zone /mean of the maximum of LV length plus the minimum of LV length. Data are representative of two independent experiments (n=4-6 per group, mean±SD, *P<0.05, **P<0.01, ***P<0.001)

Figure S2

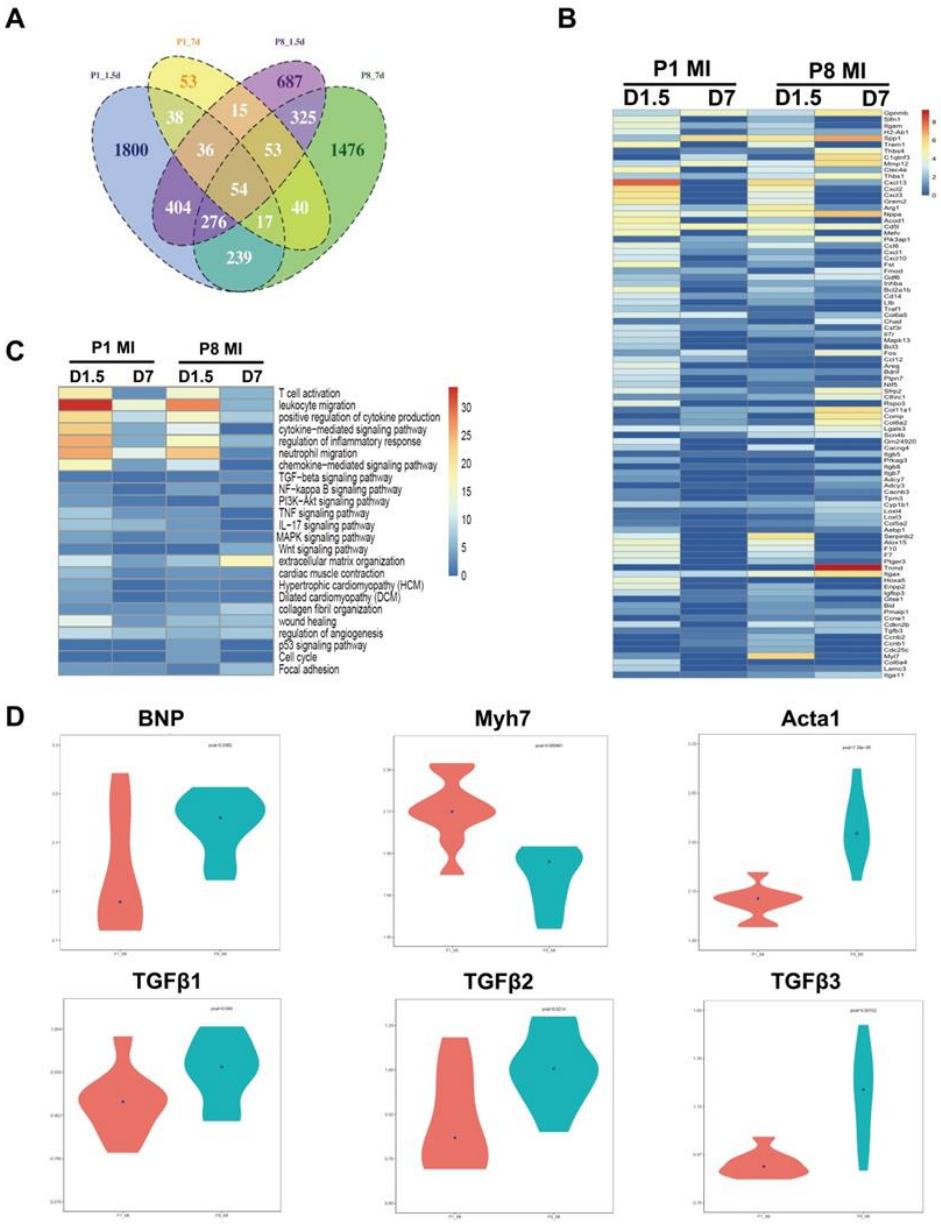

Fig S2: RNA sequencing analysis of regenerative and non-regenerative mice following MI, Related to Figure 4

(A) Venn diagram showing the overlap of DEGs among the four comparisons; **(B)** Heatmap showing log10 (fold change [F.C.]) of genes induced by MI. Fold change was calculated by comparing the transcription of each gene in MI samples over sham samples for 1.5 dpi and 7 dpi; and **(C)** heatmap showing selected top enriched GO terms and KEGG for MI inducing DEG genes; **(D)** violin plots showing selected most significantly differential-expressed genes that regulate cardiac hypertrophy and fibrosis after injury.

Transparent Methods

Animal procedures

All animals were approved by the Ethics Review Committee of Guangdong Medical University in accordance with the principles of animal welfare from the Institutional Animal Care. All animals were treated and analyzed in a blinded manner.

Drug administration

Neonatal ICR mice were intraperitoneal (i.p.) injected with DMSO or celecoxib (Selleck Chemicals) at 50 mg/kg per mouse at 0, 1, and 2 days after surgery. Mice were sacrificed at different time points after surgery.

Neonatal mouse heart cryoinjury (CI)

CI was performed as described in previous study (Yu et al., 2016). Briefly, neonatal mice at P3 or P8 were subjected to hypothermic anesthesia for 2–3 min. Mouse limbs were fixed with forceps, and 75% medical ethanol was applied to disinfect the surgical area. An incision (<1 cm) was made along the sternum and vertical of the chest muscles under a stereo microscope. After exposing the left ventricle (LV), blunt port copper wire (Area: 1 mm^2 or 2 mm^2) was frozen in liquid nitrogen and then placed on the LV (maintained time: ~5 s), an area of white frostbite appeared in the LV. After injury, the chest and skin were sewn up with sutures (8-0 and 11-0). After surgery, neonatal mice were placed under warming light. In sham groups, the same experimental procedures were performed as mentioned above, except liquid nitrogen was replaced with phosphate-buffered saline (PBS) at room temperature.

Echocardiography

Mice were anesthetized and maintained with 2% isofluorane in 95% oxygen. The LV systolic function was measured using a digital ultrasound system (VINNO6 LAB Imaging System, China) at 4 weeks following CI with echocardiography in mice. Echocardigraphic M- mode images were obtained from a parasternal short-axis view. Conventional measurements of the LV were as follows: internal diameters at end diastole (LVIDd) and end systole (LVIDs), posterior wall thickness (LVPWd and LVPWs), intraventricular septal thickness (IVSd and IVSs), end-diastolic volume and end-systolic volume (EDVs and ESVs), ejection fraction (EF%), and fractional shortening (FS%). All mentioned indexes were calculated for each mouse in a blinded manner, and nine representative contraction cycles were measured for analysis.

Quantitative Real Time-PCR (qRT-PCR)

Total RNA of heart tissue was extracted with TRIzol® Reagent (Invitrogen, Carlsbad, CA, USA). cDNA samples were synthesized with cDNA Synthesis SuperMix (Takara Biotechnology, Dalian, Liaoning, China). For qPCR, SYBR Premix Ex Taq kit (Takara Bio Inc, Dalian, Liaoning, China) was used. Each qPCR reaction (20 μL) was conducted in triplicates, and the mRNA expression levels of the genes of interest were calculated using the $2^{-\Delta\Delta Ct}$ method and normalized to the housekeeping gene GAPDH. Amplification

of cDNA was performed on a 7500 Real-Time PCR system (Applied Biosystems, Foster City, CA, USA), and the sequences of the oligonucleotide primers are shown in Table 1. The PCR conditions were as follows: 95 °C for 1 min; 40 cycles of 95 °C for 10 s, 60°C for 30 s, and 72 °C for 10 s; 95 °C for 15 s, 60 °C for 15 s, and 95 °C for 15 s.

Western blot

Heart tissues were harvested after washing with ice-cold PBS and lysed for 30 min in ice-cold RIPA lysis buffer containing protease inhibitor cocktail (Roche, Indianapolis, IN, USA) and separated by 10%–12% SDS-PAGE. After being transferred onto polyvinylidene fluoride (PVDF) membranes (Millipore, Billerica, MA, USA), PVDF membranes containing protein were blocked using 5% non-fat dried milk dissolved in TBS (20 mM Tris-HCl, 150 mM NaCl, pH 7.6) buffer supplemented with 0.1% (vol/vol) Tween-20 at room temperature for 1 h. After washing, the PVDF membranes were incubated overnight at 4 ℃ with primary antibodies: COX-2 (CST, 12282#), Snail (CST, 3879S#), TGFβ2 (SantaCruz, 374659#), VCAM-I (CST, 39036S#), ICAM-I (Novus, NBP2-22541), MCP-1 (Novus, NBP2-22115SS), and β-actin (CST, 4970s#). After incubation with secondary antibodies at room temperature for 1h, the bands were visualized with enhanced chemiluminescence detection reagents (Millipore, Billerica, MA, USA). The protein expression levels of specific gene were calculated as the relative band density to that of β-actin using ImageJ software (National Institute of Health, Bethesda, MD, USA).

Enzyme-linked immunosorbent assay (ELISA)

CI was surgically performed in the P8 heart of ICR mice treated with celecoxib and DMSO. After collecting heart tissue of infarcted/boarder zone at 1, 3, and 7 days following CI, heart tissues were homogenized for 5-10 seconds and lysed for 20 min in ice-cold RIPA lysis buffer containing protease inhibitor cocktail (Roche, Indianapolis, IN, USA). After that, taking supernates and store samples at -70 ℃. The protein level of MCP-1 was measured by MCP-1 ELISA kit (RK0038, ABconal, Woburn, MA 01801), according to the manufacturer's instructions.

Immunohistochemical and immunofluorescence analysis

Mouse hearts were perfused and fixed in 4% paraformaldehyde at 4 °C overnight. The fixed heart tissues were washed once with 30% sucrose and perfused in 30% sucrose at 4 °C for 48 h before embedding at optimal cutting temperature compound. All heart tissues were embedded in a cross-section orientation, and six micrometer frozen sections were prepared prior to staining with H&E (Maixin, Fuzhou, China), WGA-Alex 555 (Lifetech, W32464, Carlsbad, CA), and Masson's trichrome stain (Meilun, Dalian, China) in accordance with the manufacturer's instructions.

Measurement of cell surface area

All heart tissues were embedded in a cross-section orientation, and six micrometer frozen sections were prepared prior to staining with H&E (Maixin, Fuzhou, China) and WGA-Alex 555 (Lifetech, W32464,

Carlsbad, CA) in accordance with the manufacturer's instruments. All stained images (40×, 100×, 200×, and 400× magnifications) were collected under a microscope (Mshot, MF43-N, Gangzhou, China). The cross-sectional area of cardiomyocytes was calculated with a statistical analysis as previously described (Streicher et al., 2010). The size of cardiomyocytes was calculated with ImageJ software (National Institute of Health, Bethesda, MD, USA).

Flow cytometry

Heart tissues were sectioned into small fragments with sterile scissors and consequently dissociated with a mixed buffer of Collagenase, Type II (Lifetech, 17101015, Carlsbad, CA) and Dispase (Solarbio, D6430-1g, Beijing, China) at 37 ℃ for 30 min. After dissociation, the tissues were added with 10% FBS (Gibico, Carlsbad, CA) to stop the enzymatic action and washed once with PBS. Prepared dissociated single heart cells and splenocytes were incubated with 1× Red lysis buffer for 2–3 min to remove red blood cells (Solarbio, Beijing, China). The collected heart cells and splenocytes were washed once with PBS, resuspended in PBS containing 1% BSA, and then stained with fluorochrome-conjugated antibodies, including F4/80-APC (Biolegend, 123116, San Diego, USA), CD206-PE (Biolegend, 141705, San Diego, USA), and Ly6C-FITC (Biolegend, 128005, San Diego, USA). After incubation at 4℃ for 30 min in the dark, the cells were washed at least two times with PBS, and then analyzed using a BD FACS Aria II flow cytometer (Franklin Lakes, NJ, USA).

RNA-sequencing analysis

Raw count data of RNA-Seq were retrieved from the Gene Expression Omnibus (GEO) database (https://www.ncbi.nlm.nih.gov/geo) under the accession no.GSE123868 (Wang et al., 2019b). Only the data of P1 and P8 at 1.5 days and 7 days after injury were imported into R and differential gene expression analysis was performed with the R package DESeq2 (Version 1.26.0) based on the negative binomial distribution (Love et al., 2014). For each comparison, genes with more than 1 count in at least one sample were considered as expressed and were used for calculating normalization factor. Cutoff values of absolute fold change greater than 2.0 and false discovery rate less than 0.05 were used to select differentially expressed genes between sample group comparisons. Venn plot was performed with R package VennDiagram (Version 1.6.20). Differentially expressed genes from Venn plots were used for GO (Gene Ontology) enrichment analysis performed with the R package clusterProfiler (Version 3.14.3) (Yu et al., 2012), and the e-values of GO enrichment analysis in each group were used for heatmap plotting in R package pheatmap (Version 1.10.12).

Statistics

Experimental data are presented as the mean±S.D of biological replicates (n=4–6 per group) and independent experiments (n=2–3). Statistical significance between groups was calculated using a two-tailed Student's *t* test. Statistical significance was considered at $P<0.05$.

Supplemental References

Love, M.I., Huber, W., and Anders, S. (2014). Moderated estimation of fold change and dispersion for RNA-seq data with DESeq2. Genome Biol *15*, 550.
Yu, G., Wang, L.G., Han, Y., and He, Q.Y. (2012). clusterProfiler: an R package for comparing biological themes among gene clusters. OMICS *16*, 284-287.